TECHNISCHE UNIVERSITÄT
CHEMNITZ

Deutsches Zentrum
für Luft- und Raumfahrt

University of Technology Chemnitz
Faculty for Behavioral and Social Sciences
Professorship of Cognitive Psychology and Human Factors

In cooperation with the German Aerospace Center
Institute for Transportation Systems

Finding Frustration:
a Dive into the EEG of Drivers

Master thesis by:	Marie Klosterkamp
Scientific supervision & evaluation:	Prof. Dr. Alexandra Bendixen M.Sc. Esther Bosch
Contact:	Marie Klosterkamp Vettersstraße 9 09126 Chemnitz marie.klosterkamp@s2018.tu-chemnitz.de Study program: M.Sc. Human Factors Student identification number: 542085

Table of Contents

Abbreviation table

AAI	-	Alpha Asymmetry Index
BCI	-	Brain-Computer Interface
dB	-	Decibel
EEG	-	Electroencephalogram
EOG	-	Electrooculogram
ERP	-	Event Related Potential
ICA	-	Independent Component Analysis
ms	-	Millisecond
PANAS	-	Positive Affect Negative Affect Schedule
SAM	-	Self-Assessment Manikin
µV	-	Microvolt
VAD	-	Valence, Arousal, Dominance

Register of figures

Register of tables

Abstract

Emotion recognition technologies for driving are increasingly used to render automotive travel more pleasurable and, more importantly, safer. Since emotions such as frustration and anger can lead to an increase in traffic accidents, this thesis explored the utility of electroencephalogram (EEG) features to recognize the driver's frustration level. It, therefore, sought to find a balance between the ecologically valid emotion induction of a driving simulator and the noise-sensitive but highly informative measure of the EEG. Participants' brain activity was captured with the *CGX quick-30* mobile EEG system. 19 participants completed four different frustration-inducing and two baseline driving scenarios in a 360° driving simulator. Subsequently, the participants continuously rated their frustration level based on the replay of each scenario. The resulting subjective measures were used to classify EEG time periods into episodes with or without frustration. Results showed that the frequently used measure of the Alpha Asymmetry Index (AAI) had, as hypothesized, significantly more negative indices for *high frustration* (vs. *no frustration*). However, a commingling effect of anger on this result could not be dismissed. The results could not provide evidence for the yet to be replicated previous research of frustration correlates within narrow-band oscillations (delta, theta, alpha, and beta) at specified electrode positions (frontal, central, and posterior). This thesis concludes with suggestions for subsequent research endeavors and forthcoming practical implications in the form of insights acquired.

1 Introduction

In light of the seemingly inevitable climate change, a new trend appears to emerge from the accordingly adapting mobility sector. Instead of focusing on pollutive horsepower and speed as major selling points for cars, manufacturers are increasingly turning towards innovative interaction designs to excite customers for their products (Braun et al., 2020). Similarly, researchers and developers of eco-friendly and innovative mobility services such as ride-sharing and autonomous shuttles work on designing these mobility options to be more attractive and easier to use than the conventional privately-owned automobile (Cellina et al., 2019). These new approaches build on increasing the user's experience of the vehicle, thereby conveying a feeling of leading-edge technology and turning the everyday chore of commuting into a pleasure ride. Accordingly, the generally growing research interest in *affective computing* has also reached its way to the automobile (Braun et al., 2020; Torres et al., 2020). The idea behind affective computing is to regard the user's emotional state as the primary communication channel for the human-machine interaction (Alimardani & Hiraki, 2020). Besides enlarging economic growth through the elicitation of pleasant driving situations, this research, more importantly, aims at facilitating a safer driving environment, since emotions are known to impact important cognitive tasks indispensable for driving such as decision-making, judgment, and attention (Jeon, 2015). Noteworthy, it has been shown that negative emotions such as anger and frustration lead to degraded driving performance and diminished attention (Chliaoutakis, et al., 2002; Jeon, 2015; Lee, 2010). A recent survey showed that drivers experienced negative emotions mainly due to bad traffic and unforeseen hindrances on their route (Braun et al., 2018). As much as 50 % of the interviewed drivers reported wishing for an empathetic reaction of the car, by playing calming music and taking control over the navigation, and driving in an autonomous fashion (Braun et al., 2018). While playing music is easily implemented the autonomous driving has yet to fully arrive. However, before the machine can enact these techniques it must first be able to accurately infer the drivers' emotional state. To accomplish this, current research for affective automotive interaction design mainly focuses on facial expressions, tone of voice, and similar behavioral signs. Attempting to provide additional information beyond these behavioral expressions, the present study set out to complement existing efforts by exploring brain-based emotional measures. Combining emotion recognition research from affective computing and *brain-computer-interfaces* (BCIs) with the use of a driving simulator aims to provide ecologically valid results to lead the way for the development of practical applications of this technology.

Section 2 enlightens the theoretical principles of emotions (also particularly for driving), their measurement, as well as the methodology of EEG including a general overview of the brain and concludes with the derivation of the primary hypotheses.

Section 3 comprises the methodology underlying this study.

Section 4 visualizes the manipulation checks and presents the results of the analyses.

Section 5 discusses the found results, elucidates limitations, and offers implications for future research.

2 Theory

2.1 Disambiguation of emotion

In the field of psychology, scientists are accustomed to the task of translating latent, subjective experiences into manifest, measurable, and – assumed to be – comparable concepts of a person's traits and states such as emotions. The *Dorsch* encyclopedia defines *emotion* as a complex psychological state, which is responsible for initiating and accompanying goal-directed behavior and results in physiological, behavioral, and subjective changes (Dorsch & Wirtz, 2020). *Affect*, which may sometimes be used synonymous with emotion, shall for the purpose of this thesis refer to the most inclusive category whilst subsuming emotion, feelings, and moods following the approach of Jeon (2017). While Jeon (2017) defines *feelings* as representing the internal, subjective interpretation of the bodily responses he describes *moods* as more enduring, diffuse, and subtle, leading to an omnipresent but not necessarily conscious experience thereof.

2.2 Emotion models

From the common ground described above, the definition of emotions varies broadly between the three major branches of emotion models (discrete, dimensional, and constructionist) with the assumed dimensionality and the degree of variation between the representations of emotions being the most discriminative distinction between these models. Subsequently, these models will be outlined following the classification of Mishra and Tiwary (2019).

2.2.1 *Basic emotion model*

Paul Ekman and Jaak Panksepp, as prominent advocates of the discrete emotion model, assume emotions to be unidimensional and invariant across instances. In his early studies, Ekman reports having found a universality for the manifestation and recognition of emotions based on pictures of emotional facial expressions, which were similarly categorized across cultures (Ekman & Oster, 1979). Both Ekman (Ekman & Cordaro, 2011) and Jaak Panksepp (2004) view emotion categories as emerging from dedicated brain circuits activated by specific mechanisms resulting in unique mental states. Panksepp (2004) further proposes that emotions are heritable and homologous in non-human animals. When speaking of models which presume discrete emotions, the *Basic Emotion Theory* seems to be the most noteworthy. This theory, in addition to the above-mentioned assumptions, builds on research pointing towards the universality of several basic emotions. For Ekman and Cordaro (2011) these basic emotions comprise "anger", "fear", "surprise", "sadness", "disgust", "contempt", and "happiness". They further presume these seven emotions to be the building blocks for all other emotions belonging to the same "emotion family" (Ekman & Cordaro, 2011).

2.2.2 *Dimensional emotion models*

Criticizing the determinism of the discrete emotional model, dimensional emotion models assume, that emotions can be mapped into a multi-dimensional space. Two-dimensional emotion theories regularly make

use of the domains of valence (positive vs. negative) and arousal (active vs. passive) to classify emotions, which comprises the *Circumplex Model of Emotion* (Posner et al., 2005; Russel, 1980). Mehrabian (1996) expanded this model by adding a dominance (high vs. low control) axis, thereby resulting in the three-dimensional *VAD Model* (Valence [synonymous with pleasure], Arousal, Dominance Model). In their review, Al-Nafjan (2017) and his team reported that in most papers investigating EEG-based emotion recognition such dimensional models were used (172 articles, 65 %), while in 22 % the model was not specified.

2.2.3 *Appraisal and constructionist emotion models*

In opposition to the discrete and most dimensional models, some models presume emotions to vary significantly not only across contexts but also across instances of the same emotion (Gross & Barret, 2011).

Scherer (2005), an eminent supporter of the *Appraisal Theory*, subscribes five major functions to emotions which are: "regulation of the system", "preparation and direction of action", "communication of reaction and behavioral intention", "monitoring of internal state and organism-environment interaction" as well as the "evaluation of objects and events". The latter function – the evaluation of objects and events – is the central element of the appraisal theory and proposes the necessity of an antecedent cognitive evaluation prior to the genesis of emotions (Scherer, 2005).

A prominent psychological-constructionist approach is the *Theory of Constructed Emotions*, in which it is assumed that an instance of emotion is the result of the continuously modified categorization of information from sensory, contextual, and cultural sources in synchronization with prior experiences (Barett, 2017).

This view is in line with the results of a meta-analysis conducted by Clark-Polner, Wager, and Barett (2016), who found that the valence of emotional stimuli does not produce distinct patterns for negativity and positivity in the brain but is instead represented as a flexible probabilistic pattern of neurons on a voxel level. Barret (2013, 2017) further proposes, that in general, the concept of degeneracy applies to all emotional processes, meaning that for a single emotion category many different arrangements of neurons, regions, and networks can produce the same classification for the emotion category. Therefore, some scientists argue that averaging activation maps of brain activity specific to one emotion category results in a pattern that does not allow to predict any single activation pattern leading to this average (also known as an *inverse problem*) (Clark-Polner et al., 2016).

2.2.4 *Emotion models in practice*

It should be noted that all approaches to classify emotions are not discretely belonging only to one of the major three emotion models, since they can be arranged on a continuum from strictly basic emotions to the solely social constructions of emotions as was realized in the scientific article by Gross and Barret (2011). However, it seems apparent, that the assumed emotional model has a profound influence on the hypothesized intra- and interpersonal manifestations of emotions (such as frustration). For this reason, it has been suggested to treat the different perspectives as alternative explanations of the same phenomenon

and to choose an appropriate theory based on the research´s characteristics (measurement methods, tasks, and aim of the study) (Jeon, 2017; Mühl et al., 2014). While machine learning techniques provide the ability to search for emotion-related patterns purely data-driven without the need for prior theoretical assumptions, this comes at the cost of the results' explainability and replicability. In addition, even if no theoretical foundation is explicitly presumed, the choice of used features and the algorithm settings (to find one pattern or a composition of patterns) already inherit assumptions about the representation of emotions (respectively comparable to discrete and dimensional emotion models).

Hence, in the case of affective computing, researchers commonly make use of either discrete or dimensional emotion models to aggregate comparable measures across instances and individuals, so that these may be utilized as relatively simple features for classifiers to recognize distinctly different emotions (Al-Nafjan et al., 2017). As a possible antecedent to emotion recognition, this study focuses on a functional classification of emotion categories adhering to previous dimensional emotion theories and analogous self-report measures. This focus allows reducing the complexity of emotions to distinguishable categories which in turn provides the basis for assessing if the manipulation of the emotional state is in coherence with previous findings based on dimensional theories.

2.3 Frustration

2.3.1 *Definition of frustration*

According to Jeronimus and Laceulle (2020) frustration is defined as irritable distress arising if a person experiences a limitation, exclusion, or failure. Frustration hence occurs when the accomplishment of attaining a goal, or the satisfaction of a need is hindered (Dorsch & Wirtz 2020). Together with the emergence of frustration, a specific frustration-arousal supposedly arises to approach the cause of the frustration if the problem is perceived to be controllable. Otherwise, the frustration-arousal is presumed to lead to the facilitation of avoidance behavior (Jeronimus & Laceulle, 2020).

Locating frustration in the *VAD Model* of emotion (Figure 1), it is positioned on the negative side of the valence spectrum towards "displeasure" and occupies a positive arousal state tending to "excitement" (Russel et al. 1977; Mehrabian 1996; Torres et al. 2020). Frustration is differentiated from anger mainly through the inverse polarity on the dominance continuum. While anger is related to feelings of "being in control", frustration is associated with the perception of "being controlled" (Russel et al., 1977).

Figure 1 | Valence-Arousal-Dominance Model of Emotion

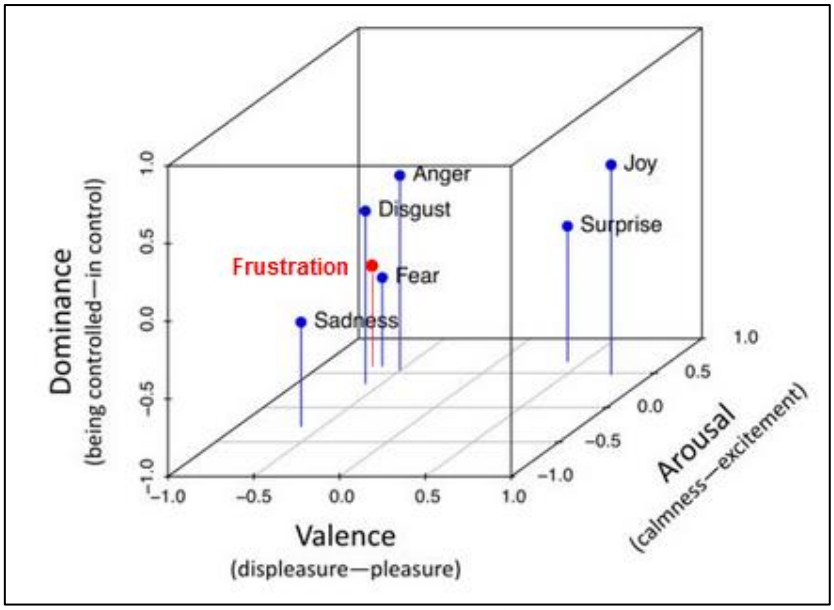

Note: this figure has been adapted from Torres et al. (2018)

For this study, no explicit assumption is made on the dimensionality of frustration for the main hypotheses since the focus is essentially on the presence or absence of this emotion. However, by following previous research locating frustration within the circumplex model for the manipulation check, the dimensional emotion model is followed.

2.3.2 *Frustration in the context of driving*

As one might remember from the first driving lessons, the act of driving an automobile is a highly complex task that requires full attention and the coordination of multiple cognitive and motor tasks. Adding to this high workload is the influence of affect on driving, which becomes apparent when thinking about the nervous mistakes made in those early lessons due to unfamiliar and potentially dangerous situations. In line with this example, Lee (2010) demonstrated that, in comparison to older drivers, young drivers were more frustrated by slow traffic while under time pressure, resulting in less attentiveness to unexpected events or even the overall roadway environment as well as keeping a consistent headway. Lee attributed the safer driving behavior to the better-developed emotion regulation of older drivers. This study can be viewed as an indicator of the importance of accounting for emotions within the driving context when aiming to design a safer driving situation.

Jeon (2015) therefore makes the case for an affect-integrated model for driving behavior research. In his model, he proposes affective processes to influence situation awareness (including e.g., perception and decision making), cognitive processes (including e.g., attention, memory, and automaticity), and most importantly the performance of the driving action itself.

Taking affect into account to enable the adaptation of the communication of the in-vehicle system to the driver's current needs and moods, has been shown to promote a safer driving behavior (Jonsson, 2009; Nass et al., 2005). Jonsson (2009), as well as Nass and colleagues (2005), demonstrated this effect for in-vehicle

voice interaction leading to improved adherence to traffic rules and enhanced attention as well as fewer accidents.

Moreover, companies are increasingly focusing on the driver's emotional status to increase driving safety and to improve the overall driving experience. For example, the company *Affectiva* uses in-cabin sensors (facial expressions and body posture) to detect indications of the driver's emotional reaction to the automobile's interface and automation features (Affectiva, 2021). The company further suggests a multitude of possible emotion-related adaptations to the car's features such as making changes to the media system of the car, e.g., modifying the music's volume according to the driver's emotional state or playing movies for the bored or upset children in the back seat (Affectiva, 2021).

Concluding, the detection of the affective state of drivers such as frustration has the potential to allow for the adaptation of the in-vehicle interaction in a way that aids to attenuate the driver's frustration by adjusting the vehicle's communication and functions to the driver's needs resulting in safer driving behavior.

2.4 Measuring emotions

Before such affective interfaces can be utilized, the recognition of emotions first needs to be precise enough to allow these systems to function. Hence, researchers studying emotion recognition, ought to ensure that they elicit and measure the desired emotion accurately.

For completeness, it first needs to be highlighted that the participants' well-being should at all times be the highest priority. Therefore, the emotion elicitation should be designed with the involvement of an ethical committee and performed in a reasonable and goal-appropriate manner. In addition, since all hereafter mentioned techniques include the measurement and handling of sensitive personal information, the data should be managed accordingly. Especially, practical implementations of affective computation but also research endeavors need to assure, that the collected data is handled in a way that safeguards the *mental privacy* of their users. The concept of *mental privacy* was proposed with these technologies in mind and includes criterions such as the accuracy and reliability of the emotion inference, as well as informing the user on which prediction was made and what it was based on (Hu et al., 2019).

While the accuracy rate is often used to evaluate the performance of the emotion recognition algorithm as the probability of making a correct classification, the error rate depicts the probability of making an incorrect classification (Torres et al., 2020). However, these measures are highly dependent on the number of possible classification categories as well as the amount of data for each case. Therefore, the accuracy rate should always be interpreted within this reference frame and be complemented with an evaluation of significance (Torres et al., 2020).

In the following, a short outline of general emotion elicitation and collection approaches will be provided.

2.4.1 *Elicitation*

Emotion elicitation techniques are typically divided into the following three major paradigms (Zhang et al., 2020).

The first paradigm uses the presentation of standardized emotional stimuli, represented by visual, auditory, or video materials (Zhang et al., 2020). Numerous databases are openly accessible with already classified content. The most prominent databases are the *International Affective Picture System* for visual stimuli, the *International Affective Digitized Sounds* for auditory stimuli, and *MAHNOB-HCI* as well as *DEAP* for video stimuli (Bradley & Lang, 1999; Lang et al., 2008; Koelstra et al., 2012; Soleymani et al., 2012). A review by Al-Nafjan and colleagues (2017) finds that when taken together, standardized stimuli were utilized for emotion elicitation in 155 of 248 (63 %) articles from the field of emotion recognition. The advantage of employing this kind of elicitation is the optimization for the replicability and comparability of the research results, making it an attractive option for emotion researchers. However, this approach also has its shortcomings regarding its ecological validity, given that the experimental manipulation is contingent on the emotional involvement of the participants (Hu et al., 2019).

In contrast to the standardized emotion elicitation, the second and third paradigms induce emotions actively by manipulation of the participants' behavior rather than the passive perception-based elicitation and thereby assure the emotional involvement of the participants (Kory & D'Mello, 2015).

The second paradigm of emotion elicitation makes use of past experiences or fictional situations and requires the participants to recall or imagine scenarios in which they felt the emotion of interest, which has been used in only 10 of the 248 studies (4 %) analyzed by Al-Nafjan and colleagues (2017).

The third paradigm builds on prepared tasks and social situations for the induction of emotions. The tasks or situations are designed in a way that naturally elicits the emotion using for example games, virtual reality scenarios, or social interactions (Zhang et al., 2020). A review found that 47 of 248 (19 %) articles had used prepared tasks or social interactions (Al-Nafjan et al., 2017). While it is reasonable that results from these studies might be better comparable to real-world scenarios, the accompanying social tasks are less controllable. Therefore, these studies might not achieve the same level of stimulus-standardization compared to research using standardized databases and hence could be deficient in their replicability. In addition, when using active elicitation, researchers should be aware of the possibility of reduced precision for the emotion manipulation as well as an increased variability between and within-subjects (Kory & D'Mello, 2015).

2.4.2 *Collection*

Since emotions are presumed to be accompanied by changes in behavioral, physiological, and subjective experience components, these fields represent the central domains utilized for the measurement of emotions. While changes in the first two domains can be observed and measured, the latter is only accessible through interoception (bodily self-awareness) and verbalization of the person experiencing the emotion. When measuring emotions, current research recommends the combination of subjective, physiological, and behavioral measures to account for concomitant artifacts (He et al. 2020).

Subjective. Because emotions are inherently subjective experiences, self-report accounts are needed to classify specific emotion-related bodily changes into categories or affective states. This is often referred to

as the ground-truth of emotion assessment and can presumably be captured through interviews, psychometric tests, or projective instruments (Dasborough et al., 2008).

When assessing emotions based on self-report, two frequently used measures are the *Self-Assessment Manikin* (SAM) developed by Lang and Bradley (1994) and the *Positive Affect Negative Affect Schedule* (PANAS) constructed by Watson and colleagues (1988).

The SAM mainly consists of three nine-point scales corresponding to manifestations on the valence, arousal, and dominance scale, which are each visualized by a manikin expressing the specific manifestation (e.g., smiling or frowning) (Dasborough et al., 2008).

For the PANAS assessment, individuals are given a list of ten positive and ten negative adjectives, for which they are supposed to report either their state or trait affect (specified by time frame) on a five-point Likert Scale ranging from "very slightly or not at all" to "extremely" (Watson et al., 1988). Furthermore, there is an extended version of the PANAS which is expanded to a 60-item scale measuring 11 specific affects (Watson & Clark, 1994).

Behavioral. Based on the assumption, that emotions are accompanied by changes in a person's behavioral expression, one can attempt to deduce an emotion from a person's facial expression, body posture and gestures, tone of voice, and numerous other bodily changes. The *Facial Action Coding System* is the most renowned approach to classify facial expressions based on the work of Ekman and Friesen (2002), who revised their first manual from 1978. This system describes specific *Action Units* derived from the activation of facial muscle groups such as frowning or raising an eyebrow. While the coding of these *Action Units* was originally done manually, today with the help of computer vision and algorithms, fully automatic software developed by *Affectiva* or *iMotion* aims for the recognition of *Action Units* and several pre-defined emotions (Affectiva, 2021; Farnsworth, 2019).

In the view of basic emotion advocates like Ekman and Cordaro (2011), behavioral measures are universal and thus an unobtrusive and objective measure of emotions. However, people are able to regulate their emotions and bodily expressions, resulting in emotional responses that can be too weak to be perceived by other humans or computer-vision-based algorithms. In this regard, most of the current research uses a multitude of behavioral measures to improve the accuracy of their emotion recognition (Dzedzickis et al., 2020).

Physiological. Physiological measures of emotion, on the other hand, are assumed to be more independent from a persons' deliberate regulation. Notable physiological measures of emotions include the *Heart Rate Variability*, *Electrocardiography*, *Galvanic Skin Response*, and the measurement of brain activity, as by the utilization of an EEG.

For example, the *Galvanic Skin Response* measurement is based on emotionally induced sweat reactions, which are measured on the skin as a variation of its electrical resistance due to the sweats' salt content (Dzedzickis et al., 2020). In 2017, Ayata and colleagues demonstrated this measure to be principally

applicable for algorithms to infer their participants' emotions with an accuracy rate of roughly 80 % for the recognition of valence and arousal.

Meanwhile, measuring the *Heart Rate Variability* through the *Electrocardiogram* for emotion recognition is based on research showing that heart activity is related to emotions through its regulation by the sympathetic and parasympathetic nervous system (Dzedzickis et al., 2020).

Though these physiological measures provide reliable and objective information, they are also affected by numerous emotion-unrelated activities and therefore benefit from the enrichment with subjective accounts or behavioral measures to affiliate them to emotion categories.

Special potential for recognition of emotions lays in technologies such as the EEG and *functional Magnetic Resonance Imaging* as these technologies can, under the right circumstances, measure emotions at the place where emotional stimuli are presumed to be processed – in the brain (He et al., 2020). For the EEG in particular, some researchers stress its potential for measuring emotions since it is comparatively affordable and allows the detection of even subtle emotional states which might not be expressed in behavioral components like facial expressions or bodily gestures (Jeon, 2015; Torres et al., 2020).

2.5 The electroencephalogram

Before diving into the specifics of measuring affect-related brain processes by means of an EEG, an introduction to the method of EEG, the brains' organization, and the associated functions for specific brain areas are provided.

2.5.1 *Introduction to electroencephalography*

Affective processes in the brain, like all other brain processes, result from the activation of specific brain circuits, which generate a subtle electrical field based on a shifting electrical charge of the interconnected neural membranes. The focus of the following paragraph is the measurement of the electrical potential over the scalp through the utilization of an EEG system. Subsequently, the specifics of related neural charges will be explained.

The first human EEG was applied as early as 1924 by the Austrian neuroscientist Hans Berger (Zhang et al., 2020). It is recorded by placing sensors, called electrodes or channels in EEG terminology, on the subject's head, which are used to measure the difference in the electric potential between the scalp electrode(s) and the reference electrode(s) (Leuch, 2019). The rationale for using references is that any noise stemming from the electrical equipment or other brain-unrelated sources will also be picked up at typical reference sites such as the earlobes, nose, or mastoids (Leuch, 2019). Thereby, subtracting the voltage at a neutral point (reference) from the voltage at scalp sensors should result in canceling out these artifacts (Leuch, 2019). Another standard way to reduce possible artifacts is the measurement of ocular movement by adding extra channels to the EEG system for the recording of an electrooculogram (EOG) to subsequently clean the EEG data based on the resulting signal, containing blinks and eye movement.

The arrangement of the channels over the scalp typically follows the *International 10-20* layout standard, wherein the distance between the electrodes is set in relation to the measurement of the midline coronal and sagittal axes of the scalp (Alarcao & Fonseca, 2019; Jasper, 1958). This assures that the layout is comparable even between different-sized heads. Therefore, it is standard practice in laboratory environments to fit the electrode cap size to the circumference of the subject's head with the center electrode being positioned based on the measurement of the head's midpoint.

Despite all countermeasures, the EEG signal will naturally contain a certain degree of noise since digital filtering cannot attenuate 100 % of the undesired signal without also distorting the EEG signal (Torres et al., 2020; Widman et al., 2015). Nevertheless, filters are essential when working with EEG data. For example, a low-pass filter (attenuating higher frequencies than a defined cut-off) is inherently set by the sampling rate of the EEG system due to the Nyquist-Shannon-Theorem (Luck, 2014). Adhering to this theorem, signals can only be reconstructed properly up to those frequencies that are half of the sampling rate, which is typically within the range from 128 Hz to 1000 Hz (Luck, 2014). In addition to this online filter, offline high- and low-pass filters, attenuating frequencies below and above a certain cutoff threshold respectively, are commonly utilized to diminish artifacts such as power line noise and sweating.

While the right laboratory settings are able to achieve a relatively clean EEG, other settings such as mobile EGG systems used in practical settings are accompanied by an increased risk of being contaminated with signals from artifactual sources. Relevant in the context of this study, the independent component analysis (ICA) represents one of the multitudes of possible artifact-removal techniques which can be used to improve the signal-to-noise ratio of the data. The ICA can be used to separate brain-based EEG data from artifactual signals by employing a complex de-mixing algorithm (Klug & Garmann, 2020). This method calculates the most likely and most predominant components that presumably led to producing the observed signal, based on the time-spatial co-occurrence of this signal at adjoining channels (Klug & Garmann, 2020). After the removal of components that are expectedly related to artifactual sources such as eye-blinks and muscle activity, the EEG data optimally contains predominantly components that represent brain-based signals.

To get an idea of where these brain-based signals are generated, a general overview of the brain's anatomy will be provided.

2.5.2 *Overview of the brain*

After forming an idea about what can be observed on the outside of the head, the focus will now turn towards the inside of the skull.

Together with the spinal cord and cranial nerves, the brain composes the human central nervous system (Carter, 2019). This system is essential for the perception and interpretation of internal and external stimuli to initiate and coordinate the body's responses accordingly (Carter, 2019).

Starting from the bottom and traveling to the top, the brain can hierarchically be divided into three major parts distinct in their form and function: the brainstem, the cerebellum or hind brain, and the cortex, also termed cerebrum (Zhang et al., 2020).

Connecting the brain to the spinal cord, the brainstem, composed of the medulla, pons, and midbrain, is mostly responsible for unconscious mechanisms such as breathing and the regulation of heartbeat and blood pressure (Carter, 2019).

The cerebellum, located towards the back of the head, is supposed to be the region in control of balancing and coordinating body movement through the integrated control of muscles and body posture (Carter, 2019).

The cortex, as the biggest brain structure, consists of two lateral hemispheres, which are connected by a bridge of nerve tracts, called the corpus callosum. In medicine and neurosciences, the cortex is usually anatomically sectioned into four regions which are originally based on the overlying skull bones (Carter, 2019). The frontal region of the cerebrum, under the forehead, is intuitively named the frontal lobe. From a functional perspective, the frontal lobe is associated with muscle coordination and expressive speech while a specific part of it, the prefrontal cortex, is associated with higher mental functions such as concentration, judgment, and emotional expression (Zhang et al., 2020). Towards the back of the head, the frontal cortex is followed by the parietal lobe. Here, sensory, speech, and language functions are assumed to take place (Carter, 2019). At the back of the head lies the occipital lobe, which receives information from visual input and hence is mainly linked to vision-related functions such as image recognition (Carter, 2019). The fourth region of the cerebrum, located at the level of the ears and composed of two areas, one on each hemisphere, is the temporal lobe. Besides playing an important part in the processing of olfactory and auditory information, the temporal lobe is also related to emotion and memory (Zhang et al., 2020). In contrast to the four outer lobes, the limbic system is positioned in the center of the cerebrum and composited of various brain structures such as the mamillary bodies, the limbic cortex, the amygdalae, the hippocampus, and the thalamus (Carter, 2019). In addition to the limbic system being associated with instinctive behavior, emotions, impulses, and survival, the belonging thalamus represents the main intersection for information traveling between the cortex and brain stem (Carter, 2019).

Taking an even more in-depth look at the cortex, two types of cells are predominant within its six layers - neurons and glia cells (Carter, 2019). Glia cells are bigger in size and important for providing structural and nutritional support to the neurons, which are sending and receiving information between each other in the form of action potentials (Carter, 2019). Action potentials are based on chemical exchange processes, causing the electric charge within the neuron to change in relation to its surrounding which then travels down the neuron’s axon to the synaptic gap (Aday et al., 2017). Here, the electric charge is communicated to the next neuron's dendrite via the release of neurotransmitters. These are trigged by the arriving action potential and cause a post-synaptic excitation in the receiving neuron (Aday et al., 2017).

If a multitude of neurons aligns in sending a signal in the same direction, called a palisade, the post-synaptic electrical charge can sum up to a change in the electrical local field that is large enough to be measured as an electric potential on the scalp (Aday et al., 2017).

This is especially true for a type of neuron called pyramid cells. These cells are always aligned perpendicular to the cortex, which makes them the predestined for changing the electric field in a way that is not canceled out before passing through the brain liquid and the skull to reach the scalp (Luck, 2014). Therefore, these cells can produce a stable electrical potential, which is projected to the scalp, where the amplification of this voltage leads to measurable brain activity in the EEG in the microvolt (μV) range (Luck, 2014).

2.5.3 *Affect in the brain*

Before looking at the interplay of brain structures that are active in affective processes of the brain, it should be mentioned that cognition and affect are two distinct while highly intertwined processes (Mishra & Tiwary, 2019). In their *cognition-affect integrated model of emotion*, Misha and Tiwary (2019) propose that cognition and affect interact within a closed-loop system of cortico-cortical and cortico-subcortical structures. This means that information travels in loops between structures within the cortex as well as between the cortex and structures deeper within the brain such as the thalamus, the amygdalae, and multiple nuclei, respectively. Moreover, Mishra and Tiwary (2019) concluded that emotions are integrated results of these processes, representing learned concepts. It was found that if affect is dominant, the context becomes less important and responses to stimuli will be quicker and vice versa if cognition is dominant the response will be slower (Mishra & Tiwary, 2019). Similarly, LeDoux (2007) contributes this faster processing to the omission of the sensory cortex in the pathway for the projected information from the thalamus to the amygdalae.

There are numerous studies investigating emotions and their manifestations within the brain, therefore the following outline can only provide a big picture view of this field.

Figure 2 shows affect-related brain areas and their associated functions, which Lindquist and colleagues (2012) have analyzed in their meta-study for the brain basis of emotion.

Figure 2 | Emotion-related brain regions according to constructionist emotion models

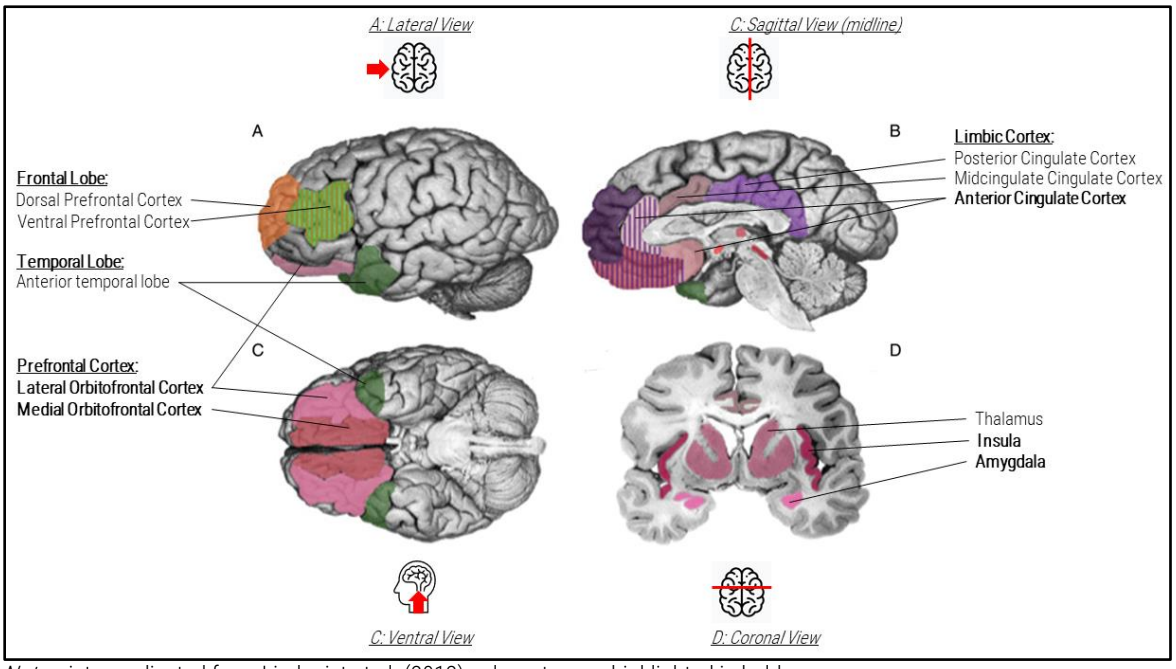

Note: picture adjusted from Lindquist et al. (2012); relevant areas highlighted in bold.

Explicitly, they found *core affect* (regions marked in pink) to be related to the activity within the prefrontal cortices, the insula and amygdalae, the orbitofrontal frontal cortex, the anterior cingulate cortex, the thalamus, and subcortical structures in the midbrain. Further, they found the limbic and prefrontal cortex to be associated with *conceptualization* (regions marked in purple), to which they presume emotions to belong.

While their results are coinciding with the constructionist model of emotions, Lindquist and colleagues (2019), for contrast, also visualized brain regions that are relevant for emotion based on dimensional and basic emotion models (Figure 3). It demonstrates the thereof presumed distinctiveness of brain regions. Thus, disgust is represented by the activity of the insula (marked in green), fear is connected to the amygdalae (marked in yellow), sadness with the anterior cingulate cortex (marked in blue), and anger with activation of the prefrontal cortex (marked in brown).

Figure 3 | Emotion-related brain regions according to basic emotion models

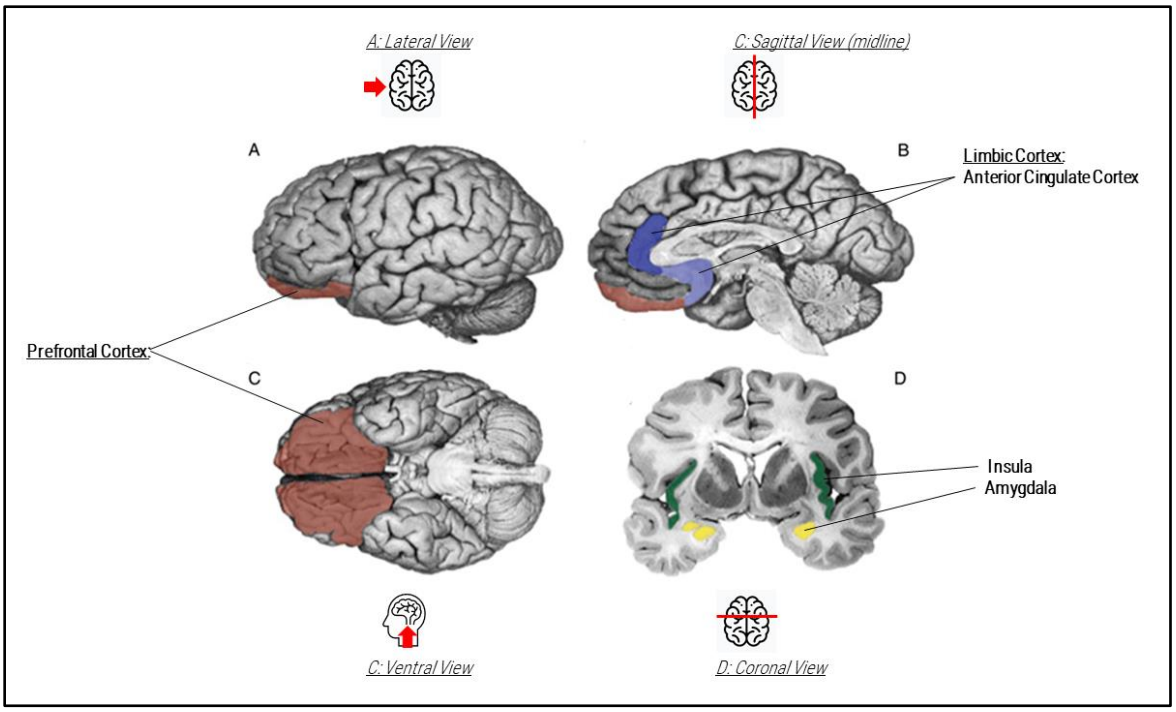

Note: picture adjusted from Lindquist et al. (2012); relevant areas highlighted in bold.

Inspecting the associated functions of the brain regions for affective processes coinciding between emotion models, activity in the insula is presumably connected to the integration of sensory information resulting in an interoceptive perception of the body as well as the emotional state (Aday et al, 2017; Lindquist et al., 2017)). In addition, the prefrontal cortex, including the ventromedial and orbitofrontal cortex, is associated with the integration of social and emotional information to construct judgments and has been termed the *affective working memory* (Aday et al., 2017; Carter, 2019; Mühl et al., 2014). The limbic system in general is often associated with affective processing, while activity in the amygdalae is regularly linked to fear and the automated assessment of threats (Aday et al., 2017; Carter, 2019). However, a meta-analysis suggests the amygdalae to be a salience- rather than a threat-detector, presuming the association to be much broader than the category of fear alone (Lindquist et al., 2012).

2.5.4 *Measuring affect with an EEG*

After previously regarding the specific brain structures associated with emotion, this section will focus on the possibility of measuring their activity with the use of EEG.

For the analysis of EEG data, a distinction between the two main types of EEG signals is essential: *spontaneous* and *evoked signals*. *Spontaneous* brain activity is an ever-present rhythmic potential fluctuation and represents brain processes regulated by the nervous system such as attention and sleep (Zhang et al., 2020). *Evoked potentials* on the other hand only occur by stimulation, as is usually the case in experimental settings. When recording an EEG, the signal will unavoidably be a mixture of both (Zhang et al., 2020). Division of these two signals can be accomplished by averaging over many stimulus trials and thus the spontaneous potential will cancel itself out since it is not correlated to the timing of the stimulus

(Luck, 2014). This is the standard approach when analyzing *event-related potentials* (ERP) (Aday et al., 2017).

EEG signals can be evaluated in either the time-domain, frequency-domain, or with a bi-spectral analysis (Zhang et al., 2020). While in the time-domain the signal is represented by the amplitude in µV typically within the millisecond (ms) range, in the frequency-domain this signal is transformed into its spectral frequencies within a certain temporal window or even over a time course, as is the case for time-frequency analyses (Torres et al., 2020).

While an EEG can provide optimal time resolution in the ms range, it is not equally accurate in the localization of the original source of the brain signal. Therefore, research for emotion detection by EEG typically focuses on the stimulus' effect on the evoked potentials over the scalp instead of localizing the neural sources of the signal (Torres et al., 2020). Within this field, the acquired signals are commonly analyzed within the frequency domain because these features are best suited for the practical application of an algorithm-based brain-computer interface (Torres et al., 2020; Mühl et al., 2014).

The frequency spectra can be acquired with the utilization of a *Fourier* transformation, which changes the original signal from the time domain into the frequency domain by estimating the amount to which the signal is comprised of specific (sine and cosine) waves (Figure 4) (Vallat, 2018). It thereby indicates the amount specific frequencies (divided into bins depending on the length of the signal) are present in the original signal as a complex number from which the phase and amplitude can be computed (Vallat, 2018). Squaring the result of the *Fourier* transformed EEG signals results in a periodogram (power spectrum), containing the squared amplitude (power) in μV^2 / Hz for each frequency of the EEG signal within a chosen time window (Vallat, 2018).

Figure 4 | Visualization of Fourier transformation

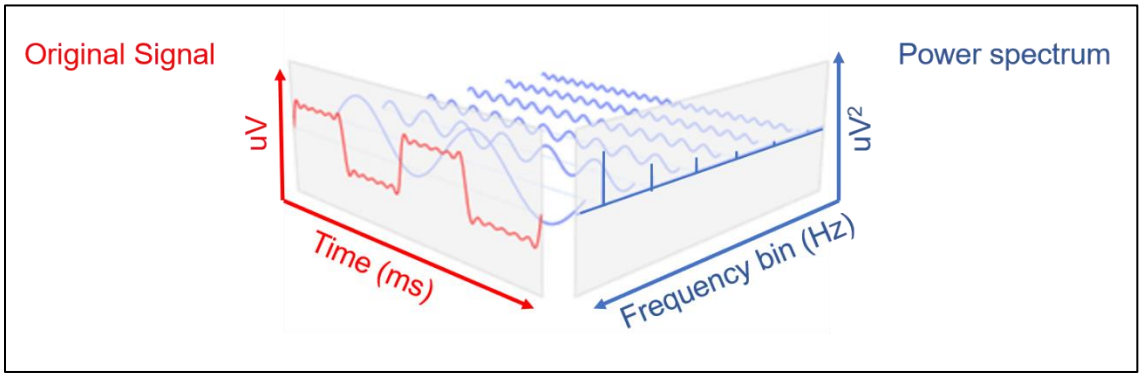

Note: picture adjusted from (Barbosa, 2013)

In EEG analysis the frequencies are typically grouped into five bands (also called bins) labeled with Greek letters: δ (delta, 0 – 4 Hz), θ (theta, 4 – 8 Hz), α (alpha, 8 – 12 Hz), β (beta, 12 – 30 Hz), γ (gamma, > 30 Hz) (Aday et al., 2017). In the following section, specific associations for the activity within these narrow-band oscillations in relation to emotion will be presented. Yet beforehand most relevant problematics of this field

need to be addressed to provide an appropriate frame for the interpretation of the associations between the measurement of neurophysiological signals and psychological features.

Firstly, the analysis of EEG data is extremely susceptible to questionable analysis choices, which could result in *p-value hacking* and *hypothesizing after the results are known*, because it provides a manifold of degrees of freedom for the analysis to explore (Ioannidis, 2005). Therefore, it is important to adhere to good scientific practices such as preregistration, using robust statistics and *p*-values adjusted for multiple comparisons in combination with further open science practices. The outreach of this issue was illustratively demonstrated by Bennet and colleagues (2009) for a different neurophysiological imaging technique (functional magnetic resonance technology), by showing that common practices lead to the detection of brain activity for a dead salmon.

Adding to this, the analysis of the observed EEG measurements is linked to the inverse problem, meaning that the same pattern can be observed due to endless combinations of vastly different brain processes (Luck, 2014). Therefore, it is indispensable to design the EEG measurement in a way, which allows to compare the results to existing literature and to distinguish the psychological construct of interest to processes that could lead to similar results (Luck, 2014).

Delta band. Activity in the delta band is mostly observed over frontal brain areas and is prominent during deep sleep (Zhang et al., 2020). Yet, there also is evidence suggesting that in wakefulness, these waves reflect reward-related brain processes as well as the detection of emotionally salient or arousing stimuli (Mühl et al. 2014; Zhang et al., 2020). Further, these waves have been found in relation to intuition and empathy processes as well as in enduring concentration tasks (Dzedzickis et al., 2020; Kirmizi-Alsan et al., 2006).

Concerning frustration, this frequency was observed to correlate with measures of frustration and valence over fronto-central regions (Lin et al., 2010; Myrden & Chau., 2017).

Theta band. This frequency is supposed to be related to the integration of affective as well as cognitive information sources and shows to be correlated with positive valence over fronto-medial regions (Mühl et al., 2014; Zhang et al., 2020). Moreover, some studies found a correlation of this band with working memory tasks, action monitoring, and response inhibition (Kirmizi-Alsan et al.,2006; Mühl et al., 2014).

For central and frontal regions this frequency was demonstrated to correlate with ratings of frustration (Myrden & Chau, 2017; Reuderink et al., 2013). In addition, midline theta power was found to relate to changes in the pleasantness of emotions (Sammler et al., 2007; Zhao et al., 2018). Moreover, frontal theta oscillations were also found to correlate to valence and arousal ratings (Reuderink et al., 2013).

Alpha band. Alpha activity is usually dominant over occipital and parietal regions of the brain (Alarcao et al., 2019; Zhang et al., 2020). It is supposedly most prevalent when the eyes are closed and decreases with the presentation of visual and auditive stimuli (Zhang et al. 2020). Alpha power is presumed to be correlated with inhibitory control, which is understood to be important for the regulation of motivational and emotional

drives (Knyazev & Gennady, 2007). Moreover, alpha activity has also been found to increase with the presentation of angry in comparison to happy faces (Güntekin & Basar, 2007).

Previous research has found correlations of these oscillations over parietal regions relating to valence (Koelstra et al., 2012). In addition, the alpha band was demonstrated to correlate with frustration ratings over posterior regions of the brain (Myrden & Chau, 2017). Furthermore, increased activity over left-sided frontal regions was observed for higher frustration ratings which relating to the frontal alpha asymmetry (Reuderink et al., 2013).

Alpha Asymmetry Index. The most frequently used method for measuring emotions within the alpha frequency range is the calculation of the frontal *Alpha Asymmetry Index* (also *lateralization effect*) (Smith et al., 2017). It is based on the difference in the activation measured at frontal electrodes, most commonly F3 and F4, thereby comparing activity over the left and the right hemisphere of the brain (Smith et al., 2017). It has been shown that topographic EEG measures of power within the alpha frequency are inversely related to the activation of local brain activity (Cook et al., 1998). Accordingly, activation of the right frontal lobe would be reflected in a decrease in alpha oscillations at related electrode positions. Hence, researchers in this field speak of a *relative left* frontal activation for a positive AAI and *relative right* activation for negative indices (Harmon-Jones & Gable, 2018).

Numerous studies have used the AAI as an indicator for emotion-related state and trait measures, analyzing mood inductions, alterations, and dispositional mood (Smith et al., 2017; Palmiero & Piccardi, 2017). Initial studies exploring the AAI propose lateralization effects of frontal brain activity to be mediated and moderated by the motivational direction approach underlying emotion (Davidson, 1993). This view has been widely adopted and some researchers have shown approach-related emotions to be associated with increased activity of the left prefrontal cortex and accordingly an increased activity in the right prefrontal cortex for withdrawal-related emotions (Sutton & Davidson, 1997; Harmon-Jones et al., 2006).

Likewise, the Index is hypothesized to occur in correspondence to a shift in the valence dimension, with greater activation of the alpha band found in left frontal electrodes in comparison to right frontal electrodes for increasing negative valence (Huang et al., 2012; Smith et al., 2017).

Furthermore, the lateralization effect has been linked to the emotional representation of the locus of control (dominance dimension). When not feeling *in control* of the situation, the EEG is assumed to show greater activation in the alpha band for the right frontal electrode (F4), and vice versa a greater activation for the left frontal electrode (F3) when feeling *in control* (Schuster, 2014; Reuderink et al., 2013).

Moreover, recent approaches highlight the ascribed inhibitory relation of the alpha oscillations to brain activity and transfer this characteristic to the AAI (Palmiero & Piccardi, 2017). It was shown that trait measures such as depression and addiction are correlated to the reduced activation of the left and right hemisphere, respectively, thereby resulting in a relative increase of alpha power in comparison to the activity of the contrary side (Cisler & Koster, 2010; Goldstein and Volkow, 2011).

As these diverse associations emphasize, the establishment of a distinct emotion-related state correlate of the AAI is still controversially debated. Yet, an agreement can be found for the fact that the emotional dimensions themselves are highly intercorrelated, as positive affect is often related to approach motivation and negative affect to the withdrawal motivation from a stimulus or situation (Harmon-Jones & Gable, 2018; Reuderink et al., 2013). Attempting to disentangle the effect of this interaction, research has demonstrated that the dominance dimension of emotion and the motivational direction approach as a state measure are the most likely candidates for effecting the frontal asymmetric brain activity (Reuderink et al., 2013; Schuster, 2014; Palmiero & Piccardi, 2017).

Nevertheless, a relatively recent review of underlying effects for the frontal lateralization concludes that, while the lateralization effect seems to be correlated with stimulus valence and approach vs. withdrawal motivation, it is also dependent on additional variables such as age and sex of the participants as well as the interaction of affect and cognition (Palmiero & Piccardi, 2017).

Beta band. Beta rhythms are frequently observed over frontal and central regions of the brain and are associated with the generation of solutions, alertness, and a focused state of the mind (Alarcao et al., 2019; Zhang et al., 2020). This frequency band has also been shown to correlate with self-induced emotions on the valence poles (Torres et al., 2020). Further, it has been demonstrated that beta rhythms decrease with the conscious experience of emotions in comparison to stimuli that did not induce a conscious emotional experience (Mühl et al., 2014; Dan Glauser & Scherer, 2008).

Importantly, this frequency band increases with the activation of facial muscles, which are involved in emotion expressions like smiling and frowning (Goncharova et al., 2003; Soleymani et al., 2016).

Previous studies have found midline beta oscillations to correlate with high ratings of dominance as well as central beta to be related to changes in the degree of frustration (Myrden & Chau, 2017; Reuderink et al., 2013). In addition, central beta oscillations have been found to correlate with valence, arousal, and liking (Koelstra et al., 2012).

Gamma band. The gamma-band is assumed to play an important role in cognitive activities and high-level functions such as integration and feedback of information (Zhang et al., 2020). In addition, a correlation with gamma waves was observed for positive as well as multi-sensory stimuli, and likewise for memory and attention tasks (Torres et al., 2020). The gamma-band has been found to correlate to valence over parietal-central, temporal, and fronto-central regions (Koelstra et al., 2012).

2.6 Previous Studies

Recognizing relevant previous research for the present thesis, selected noteworthy studies are highlighted in this section.

For one, the research team around Reuderink (2013) designed an active elicitation study to explore previously reported EEG correlates to changes in the emotional dimensions of valence, arousal, and dominance. The dimensions were manipulated through the elicitation of frustration employing a specifically designed adaptation of the “Pacman” game, which was irresponsive for 15 % of the participants’ input during

the frustration condition (Reuderink, 2009). The ratings for the VAD dimensions were collected after each trial block utilizing the SAM. As features, they used the data of an EEG system down-sampled to 128 Hz with 32 active electrodes, for which the band power of delta, theta, alpha, and beta, as well as the AAI, was calculated. Their results showed, among other effects, a significant correlation of reported valence with the AAI in the lower alpha range, yet also an even stronger correlation for the AAI in higher alpha ranges with reported dominance ratings (Reuderink et al., 2013). Furthermore, the researchers found significant correlations for valence with right fronto-central theta power as well as significant changes of power in relation to arousal for right frontal alpha and right parietal delta (Reuderink et al., 2013). Importantly, the team also found the frustration condition to be significantly correlated to alpha-band oscillations at frontal and central single electrode sites (F3, FC1, CP1, Fz).

Another relevant study for frustration detection by EEG was conducted by the researchers Myrden and Chau (2017). Their study was designed to evaluate the possibility of monitoring changes in emotional states (namely: attention, fatigue, and frustration) based on different machine learning algorithms utilizing the data from a 15-channel EEG. Their participants performed three mental tasks (arithmetic, anagram, and grid-recall), for which the difficulty was randomized on five levels from "very easy" to "very hard / impossible" (Myrden & Chau, 2017). Frustration was intended to be induced by the direct performance feedback after each task, for which the participants subsequently also rated their level of frustration on a five-point Likert scale. Notably, the participants were instructed to move as little as possible except for the end of each task to input their answers. The researchers both compared the effect of specific electrode regions (frontal, central, and posterior) as well as the accuracy between participant dependent and independent approaches. They observed that iteratively leaving out one of the three regions of electrodes did not lead to significant changes in the accuracy of frustration detection. For participant-dependent as well as -independent classification, they achieved around 71 % accuracy with a balanced dataset and three classes. For the independent set, they observed features from frontal delta and theta (Fz), posterior alpha (POz & P2) as well as central (Cz & C1), and frontal beta (Fz & F2) to be most informative for their algorithms to classify frustration. In addition, for the participant-dependent algorithm, the power at posterior (POz & P2) alpha seemed to have been most informative, while frontal (Fz & F2) delta and theta as well as overall beta possessed less importance for the recognition of frustration.

2.7 Research hypotheses

The AAI will be analyzed for its potential as a practical measure to find correlates of frustration in EEG data. According to recent research (Reuderink et al., 2013; Schuster, 2015; Smith et al., 2017; Harmon-Jones & Gable, 2018), positive stimuli and high dominance manifest in increased activity of electrodes positioned over the left frontal hemisphere. For frustration as a negative state associated with low dominance, an increase in relative left frontal alpha band activation is expected (Table 1).

Table 1 | Hypothesized characteristic of the Alpha Asymmetry Index

	No frustration	High frustration
Valence	Neutral	Negative
Dominance	High perceived control	Low perceived control
		Result in:
Alpha band activity		Left frontal increase (F3)
AAI		H_{AAI}: Negative indices

Due to the assumed relation between alpha band power and the specific manifestation on the dimensions of valence and dominance (Table 1) the following hypothesis will be investigated:

H_{AAI}: *The frontal alpha band asymmetry index will be smaller, with higher relative left activation, when frustration is rated high in comparison to a rating of no frustration being present.*

Further hypotheses (Table 2) build up on the thematically relevant research of Myrden and Chau (2017). They found the tabulated electrode-locations of the hypotheses H_{F1} - H_{F4} to possess informational importance for their subject-independent machine learning algorithm to correctly classify frustration in their EEG dataset. In concordance, H_{F1} assumes a correlation of the participants' continuous frustration rating, dichotomized in *no* vs. *high frustration*, with changes of relative power in the delta band at frontal electrodes. Likewise, H_{F2}, H_{F3}, and H_{F4} propose a correlation with the frustration classification to be found with changes of relative power in frontal electrodes for theta-band activity, posterior electrodes for alpha-band activity, and central electrodes for beta-band activity (Table 2).

Table 2 | Assumed correlates of frustration at specific electrode positions

	Delta	*Theta*	*Alpha*	*Beta*
Frustration classification *(No vs. high frustration)*	H_{f1}: frontal	H_{f2}: frontal	H_{f3}: posterior	H_{f4}: central

3 Methods

3.1 Data collection

The experimental design was built up out of two different scenarios each consisting of three simulated driving conditions with one baseline and two frustration inducting trials. In the first scenario, the participants were actively driving the car while the traffic and time pressure was manipulated within the three conditions of this scenario. The second scenario consisted of the participants driving in an automated vehicle with the frustration being manipulated by the interaction of the participants with an onboard touchscreen interface while also under time pressure. Each participant experienced the six drives in random order based on the balanced Latin square. After completion of all drives, the participants rated their frustration level for each drive continuously over the entire duration and by means of a global frustration rating for each trial.

3.1.1 *Participants*

Nineteen healthy participants, all possessing a valid driver´s license, had their EEG recorded within the experimental study conducted at the *German Aerospace Center* in Brunswick. All participants gave written informed consent to partake in the study. As reimbursement for their time, participants received 5 € per commenced half hour. The collected data was handled and saved in line with the *European General Data Protection Regulation*.

One participant was excluded from the analysis because the EEG system was too small for this participant's head size leading to highly inaccurate electrode placements and an unsuitably noisy EEG recording. Another participant's exclusion was owed to extremely low frustration ratings indicating that the frustration induction was not effective for this person.

The analysis is therefore based on the data from seventeen participants with ages ranging from 21 to 59 years (M = 33.12, SD = 13,96) of which 3 (18 %) were identifying as female and 14 (82 %) as male.

3.1.2 *Experimental setup*

To attenuate the effect of biases, such as social desirability, on the outcome of this experiment, the participants were told the cover story that the experiment was aiming to analyze the differences in eye movement and fixation between manual and autonomous driving. After completion, they were enlightened about the true nature of the study.

3.1.2.1 *Frustration induction*

For the induction of frustration within participants, the study focused mainly on two components for the elicitation of frustration: time pressure and the hindrance of achieving a goal. Previous studies have shown the effectiveness of these two components to induce frustration in the context of driving (Ihme et al. 2018). To evoke real stakes, the participants were instructed by the experimenter that 2 € would be deducted from the reimbursement for partaking in the study (10 € per hour) if the participant would not complete the instructed tasks (each task equals one of the six driving conditions) in time. In addition, participants were asked to emotionally delve themselves into the fictional stories framing each driving scenario.

Manual driving scenario. Within the manual driving scenario, participants received a phone call from their friends standing in front of the cinema, telling them that they are waiting for the participant who allegedly possesses the tickets. For the baseline drive, the participants were told by their fictional friend, that there was plenty amount of time to get to the cinema since the friends were also still on their way. In the two frustration drives, however, the friends emphasized that the movie was about to start and that they were anxiously waiting for the participant to arrive. For the two frustration drives, there were three hindrances on the way to the cinema. Two hindrances were realized by slowly driving vehicles in front of the participants, which could not be passed due to oncoming traffic. The third hindrance consisted of a left turn at a traffic signal which only allowed one car to turn during a green phase, while five cars were ahead of the participant. Adding to this, the last vehicle in front missed its time to turn, causing even more delay for the participant.

Manipulation differentiation between the two frustration drives was merely implemented by the time spacing in between the hindrances. However, to keep the participants blind to the experiment's aim, the type of virtual car and track were changed.

Time pressure was implemented by a digital countdown within the dashboard of the car indicating the time, by which the task needed to be completed. Participants were told that the countdown was set to the average time previous participants had needed for the task, when in fact the time was chosen in a way by which the participants were barely missing their target (for the frustration drives). In the baseline drive, the countdown was set to double the time which the course would take, and no obstacles were hindering the participants from achieving their task in time. In addition, during the time of the drive, the participant received an additional phone call from the friends to again induce time pressure.

Autonomous driving scenario. For the scenario of the automated drives, the participants had to perform different tasks on the user interaction display of the dashboard while the virtual car was driving autonomously. In the baseline drive, the participants' task consisted of the interaction with an easily accessible website on the user interface, ultimately resulting in several instances of pressing "continue" to reach the next page.

In the case of the two frustration drives of this scenario, the interface was designed in a way to elicit frustration through its unintuitive interaction design. The main menu consisted only of buttons with misleading labels and ambiguous symbols. Moreover, when pressing the wrong button, the participants had no way to navigate backward, resulting in the forced necessity to click through the entire options pathway before returning to the main menu.

While in one condition of the frustration drives, the participant was on the way to a meeting when receiving a phone call from their boss stressing that the participant was required to attend an important meeting at a different destination. As a result, the participant was ordered to quickly change the address within the navigation system to get to the new address on time. In the other condition, the participant was told to immediately join a conference call with important clients over the unintuitive interface.

Time pressure in the frustration drives of this scenario was implemented through a phone call from the participants' boss, stressing the important timeliness of this task.

3.2 Materials

3.2.1 *Simulator*

The experiment was conducted in a 360° virtual reality driving simulator of the German Aerospace Center in Brunswick (Fischer et al., 2014).

Participants were driving in a physically realistic car surrounded by a 360° canvas, on which six circular arranged beamers rendered the virtual driving scenarios (Figure 5). The mock-up car included all typical driving-related mechanisms (steering wheel, pedals, dashboard, etc.) and was used to navigate within the virtual driving scenario (Virtual Test Drive, Vires Simulationstechnologie, Bad Aibling, Germany).

Figure 5 | Simulator setup

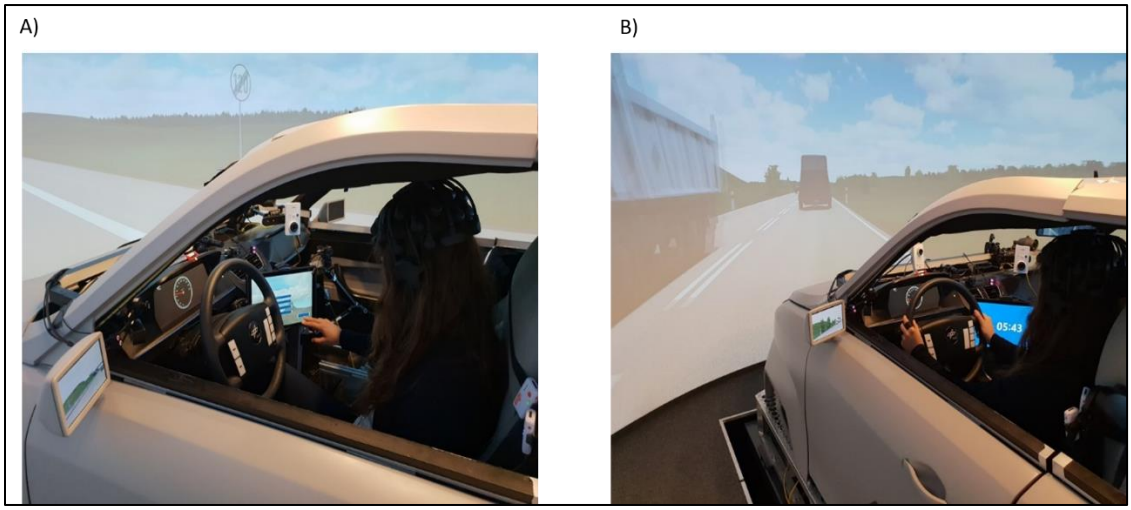

Note: A) autonomous driving scenario, B) manual driving scenario

3.2.2 *EEG system*

The "CGX quick-30" mobile EEG system from CGX (formerly known as *Cognionics)* with a 29-channel layout was utilized to capture the participants' brain activity. The channel locations adhere to the extended international 10-20 layout and can be seen in figure 6.

Figure 6 | Channel locations of the "CGX quick-30" mobile EEG system of CGX

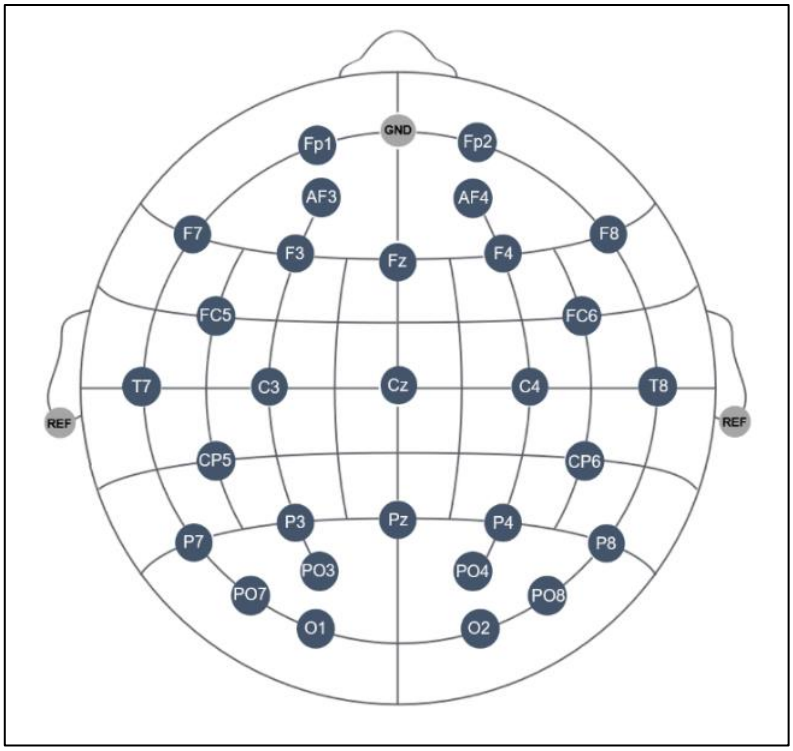

Note: this figure was adapted from cgxsystems.com

The system uses active dry electrodes and samples at a rate of 500 Hz. The ground electrode of this system is positioned in the middle of the forehead between the Fp1 and Fp2 electrodes. The reference channels in this study were placed at the earlobes.

3.2.3 *Subjective rating*

Subsequently to concluding all drives within the simulator, the participants continuously rated their frustration level based on an over-the-shoulder video of their recorded driving sessions. The acquisition of the continuous frustration rating was realized by the use of a joystick controller, which the participants were instructed to push away to the degree (0 – 100 %) they felt frustrated in concordance to the situation seen in the video of their drive. Their current frustration rating was visualized for the participant to be seen next to the video. The joystick would jump back to its zero position if it was not actively pushed. The resulting subjective measure was used to classify EEG time periods as frustration present or absent.

In addition, participants filled out a questionnaire compromised of adjusted PANAS items including a total of 22 emotional adjectives to be rated for each drive. The adjectives were to be rated based on how well these represent the affective state of the participant during each of the six drives based on a five-point Likert scale from "very slightly or not at all" to "extremely". Whereas 16 of these adjectives, based on the original PANAS version (Watson & Clark, 1994), the items "frustration", "anger", "sad", "surprised" and "relaxed" were added to be used as control measures for the frustration induction.

Further, the participants were asked to rate their valence, arousal, and dominance based on a five-point Likert scale. For valence, the scale reached from *negative* (1) to *positive* (5), for arousal from *excited* (1) to *calm* (5), and for dominance from *influenced* (1) to *independent* (5).

3.2.4 *Software*

Processing of the EEG data was accomplished by the use of *Matlab 2019b* (The MathWorks, 2019) complemented with the *Signal Processing Toolbox* (version 8.3) in combination with *EEGlab* (version 2021.0; Delrome & Makeig, 2014). Statistical analysis was conducted in *SPSS* (version 21) while diagrams were created in *R Studio* (version 1.2.5019) (RStudio Team, 2019).

3.3 Pre-processing

Figure 7 illustrates the pre-processing procedures, which will be elucidated in the following.

Figure 7 | Pre-processing workflow applied using Matlab and EEGlab

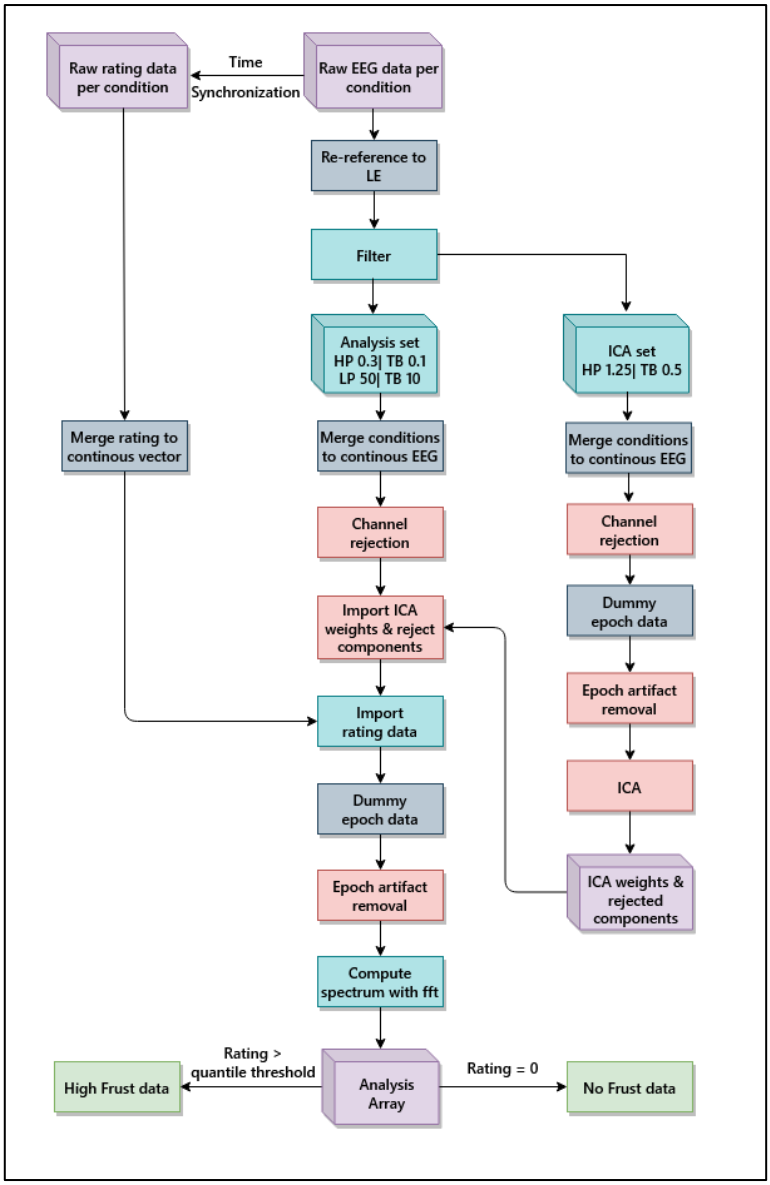

Note: LE = linked earlobes HP = high-pass filter, LP = low-pass filter, TB = transition bandwidth

3.3.1 *Re-referencing*

As a first step, the online EEG data referenced to the right earlobe was offline re-referenced to the averaged earlobes to prevent a lateral bias in voltage distribution and generate comparable results for analyzing lateralization effect as suggested by Leuch (2019).

3.3.2 *Filtering*

As visualized in figure 7, two different filter designs were employed during the processing of the EEG data, one for the ICA set and the other for the analysis data set. This is due to the fact that the ICA decomposition is sensitive to noise within the high-frequency range and therefore a more conservative threshold for the high-pass filter is needed (Klug & Gramann, 2020). Klug and Gramann (2020) suggest the filter cut-off for ICA decompositions with data from mobile EEG systems to be greater than 1 Hz while

sustaining from the use of low-pass filters. Therefore, the high-pass filter cut-off frequency for the ICA set was specified as 1.25 Hz with a 0.5 Hz transition bandwidth. No low-pass filter was employed for this set.

For the analysis data set a 0.3 Hz cut-off frequency was deployed for the high-pass filter with a 0.2 Hz transition bandwidth as well as a lowpass filter with a 50 Hz cut-off frequency and a 10 Hz transition bandwidth following the filter settings of previous research (Reuderink et al., 2013; Schuster, 2014).

For both sets, a *zero-phase Hemming window sinc FIR filter* with a maximal passband deviation of 0.0022 (2 ‰) and a 53 dB (decibel) stopband attenuation was realized by the *firfilt* function (version 2.4) from *EEGlab* (Delrome & Makeig, 2014).

3.3.3 *Merging of conditions*

The formerly divided continuous EEG recordings and frustration ratings for each of the six drives were merged into one long dataset per participant. This allowed for the independent component analysis to be utilized only once per participant instead of six separate analyses with the satisfied prerequisite that the EEG setup is identical for all drives.

3.3.4 *Channel rejection*

To remove bad data from artifacts of individual channels due to for example the displacement of electrodes or inadequate scalp contact, the *clean_rawdata* function (version 2.3) was deployed in EEGlab (Delrome & Makeig, 2014). The function was exclusively used for the removal of bad channels without the removal of bad data segments via the *artifact subspace reconstruction* algorithm. Channels were rejected if they were flat for more than five seconds, they correlated less than 80 % with the neighboring channels or the high-frequency noise passed a threshold of four standard deviations. Removed channels for each participant can be viewed in appendix B.

3.3.5 *Epoching data*

After the channel rejection, the data was epoched into one-second segments for further artifact removal processes as well as for the computation of the channel spectra. The events used for this epoching were merely dummies events occurring every full second.

3.3.6 *Epoch rejection*

To remove epochs with a low signal-to-noise ratio, the EEGlab functions *jointprob*, *kurt,* and *deltrej* were used. Epochs were rejected when within or between channels, the standard deviation of the probability or kurtosis of the signal was higher than five standard deviations. In addition, a delta criterion of ± 250 µV amplitude deviation of the channels within an epoch was used to exclude noisy data from analysis using the *eeg_rejdelta* function (Widman, 2006). The threshold, which is higher than the conventional ± 100 µV threshold, was chosen based on the tradeoff between the signal-to-noise ratio and the amount of data remaining for analysis. A detailed table of the trade-off can be viewed in appendix A. The conventional 100 µV threshold would have led to the exclusion of 6 participants (35 %) due to undercutting a previously set

limit of at least one minute of accumulated data for each participant following the suggestions from Tower and Allen (2009) for finding reliable results regarding the AAI.

3.3.7 *Independent component analysis*

In addition to the rejection of artifacts within epochs or channels, an ICA with the *runica* algorithm was realized to remove artifacts such as muscle activity, eye movements, and blinks (Delrome & Makeig, 2014). The manual classification was performed in unison by two researchers coming into agreement about the rejection of artifact-laden components. In addition to the manual classification of the components, the function *IClabel* (version 1.3; setting "Lite") was used as a substitute for an independent judgment. It classified components based on the probability (> 80 %) for comparable data to be labeled as muscle or eye artifacts by experts. The resulting rejection matrix was then transferred and applied to the analysis data set. The number of rejected components per participant is reported in appendix B.

3.3.8 *Frustration classification*

As previously described, the continuous frustration rating of the participants for each drive was merged into a continuous rating over all six drives. It was then added as an additional channel to the EEG data prior to the epoch rejection, so it could be accessible for the classification of each epoch even after the rejection of artifact-laden epochs. Thereby, the mean rating over the one-second time interval of the analyzed epoch could be extracted concurrently with the feature extraction. In the next step, the 0.6 quantile for each participant was calculated and then used to classify the epoch as *high frustration* if the mean frustration rating of the epoch was higher than the participant-dependent quantile threshold. Analogously, if the mean frustration rating was zero, the epoch was classified as *no frustration* being present. The data in between those thresholds was disregarded for the analysis. The mean quantile threshold across participants was 0.37 with a total of 12986 *no frustration* and 3048 *high frustration* epochs.

3.3.9 *Feature extraction*

The analysis was conducted within the frequency domain of the EEG data, for which a fast *Fourier* transformation was used to decompose the EEG data into frequencies for a fixed window size of one second, for which length of data points was zero-padded to the next power of two (512 pts), resulting in a periodogram with a one Hz resolution. The absolute power (in μV^2) of the frequencies was then approximated using the composite *Simpson´s rule* utilized by the *simps* function (version 1.5.0.0).

For the analysis, the absolute power within each frequency was then divided by the total power of the spectrum (2 - 45 Hz) resulting in the relative power, which was transformed to a logarithmic scale (natural logarithm) to achieve a normal distribution for the resulting measure, following the recommendation of Smith and colleagues (2017).

$$Measure = \log\left(\frac{absoulte\ power\ in\ frequency\ band}{power\ of\ entire\ spectrum}\right) = \log\left(\frac{\mu V^2\ in\ \delta/\gamma/\alpha/\beta}{\mu V^2\ in\ 2-45\ Hz}\right)$$

Alpha Asymmetry Index. For the scores of the AAI, the relative spectral power for the alpha band (8 – 13 Hz) was calculated according to the process described above. The resulting measure at electrode F4 was then subtracted by the corresponding measure at F3 within the same epoch and divided by the overall activity of both electrodes.

$$Frontal\ Alpha\ Asymmetry\ Index = \frac{F4 - F3}{F4 + F3}$$

Frequency-related changes. For analyzing changes of the relative power in specific frequency-position pairs in relation to frustration, the mean over all channels of the corresponding area was calculated as the final measure. Table 3 shows the specific channels used for each frequency. In case of missing channels, due to the rejection of such during pre-processing, the channel information was not interpolated, instead, the mean was summed over one less channel for this participant. The missing channels per participant are found in appendix B.

Table 3 | Channels used for feature extraction

Frequencies		Channels
Delta	(2- 4 Hz)	Fz, Fp1, Fp2, F3, F4
Theta	(4- 7 Hz)	Fz, Fp1, Fp2, F3, F4
Alpha	(8- 13 Hz)	Pz, P3, P4, PO3, PO4
Beta	(13- 30 Hz)	Cz, C3; C4

3.4 Statistical tests

Within each driving scenario, the data from both drives designed to induce frustration were treated as one condition (*frustration drives*) and compared against its *baseline drive*.

For the Alpha Asymmetry Index, one-sample *t*-tests (one-sided) were used to find significant changes between the epochs rated *high* in frustration in comparison to epochs rated as *no frustration* present based on the one-second mean of the originally continuous frustration rating of the participants per scenario (autonomous vs. manual). The *t*-tests were one-sided based on the directedness of the hypothesis, expecting higher AAI indices for *high frustration* in comparison to *no frustration*.

The changes between the relative power of frequency-position pairs were analyzed by calculating repeated-measures ANOVAs. The first ANOVA focuses on changes due to the frustration rating, the other on differences between the conditions within each scenario. For the first ANOVA the dependent variable was the relative power and the within-subject measures were defined as frequency band (*delta, theta, alpha*, and *beta*), use-case (*manual* vs. *autonomous*), and frustration rating (*no* vs. *high frustration*). Likewise, the second ANOVA (post-hoc) analyzed differences between the relative power (dependent variable) at specified

electrode positions for the independent variables of frequency band (*delta, theta, alpha,* and *beta*), use-case (*manual* vs. *autonomous*), and condition (*baseline* vs. *frustration drives*).

4 Results

4.1 Manipulation check

To determine if the frustration induction was successful for the experimental conditions, the mean scores for the domains of valence, arousal, and dominance are compared by an ANOVA between conditions (*baseline* vs. *frustration drives*) and use cases (*autonomous* vs. *manual*) in table 4.

Table 4 | Manipulation check for condition and use cases based on VAD ratings

Condition	*Baseline*		*Frustration drives*		ANOVA		
	M	*SD*	*M*	*SD*	*F*	*df*	*p*
Valence	*3.24*	0.17	2.67	0.12	7.231	(1, 96)	**.008****
Arousal	3.30	0.19	2.82	0.12	5.269	(1, 96)	**.030***
Dominance	*3.03*	0.22	2.34	0.13	8.219	(1, 96)	**.005****
Use case	**Autonomous**		***Manual***		**ANOVA**		
	M	*SD*	*M*	*SD*	*F*	*df*	*p*
Valence	*2.80*	0.13	2.92	0.16	0.651	(1, 96)	.422
Arousal	*3.12*	0.15	2.84	0.15	1.763	(1, 96)	.207
Dominance	*2.34*	0.14	2.80	0.18	2.995	(1, 96)	.087

Note: N = 17; Means(M) and standard deviations (SD) and results of the analysis of variance (ANOVA) for valence: negative (1) to positive (5), arousal: excited (1) to calm (5), dominance: influenced (1) to independent (5) per condition and use case

The means for the valence and arousal domain are in coherence with the assumed positioning of frustration in the *Circumplex Model of Emotion* (Posner et al., 2005), showing that participants are reporting significantly more negative and excited feelings for the frustration drives, respectively (Table 4). For the dominance domain, scores were significantly higher in the baseline drives, indicating that participants felt less *in control* in the frustration drives. There are no significant differences for the VAD ratings between the two use cases, while nevertheless, a trend towards higher dominance and lower arousal is visible for the manual driving scenario. This indicates that, following the *Circumplex Model*, the frustration induction was successful.

Assessing the validity of the frustration rating per drive through partial correlation with the VAD ratings shows a significant change for valence and dominance ratings concerning the mean frustration rating per drive as well as a high intercorrelation of the VAD dimensions (Table 5). With an increasing mean frustration rating, the participants reported having felt significantly more negative affect and less *in control* for the corresponding drives.

Table 5 | Partial correlations of the VAD domains and the mean frustration

	Valence	Arousal	Dominance
Valence	-		
Arousal	**.346*** **	-	
Dominance	**.417*** **	**.520*** **	-
Frustration rating	**- .251***	-.113	**-.250***

Note: * $p < .05$; ** $p < .01$; *** $p < .001$; frustration rating was averaged per drive; correlations were controlled for participants

Furthermore, to check the validity of the continuous frustration ratings, it was compared to the adjusted-PANAS items for frustration and anger between *baseline* and *frustration drives* within the two use cases. Based on one-sample *t*-tests, there is no significant difference between the overall adjusted PANAS ratings for frustration or anger between the use cases, though the continuous frustration rating is significantly higher in the autonomous driving scenarios ($p = .009$) (Figure 8).

Figure 8 | Frustration and anger ratings between use cases

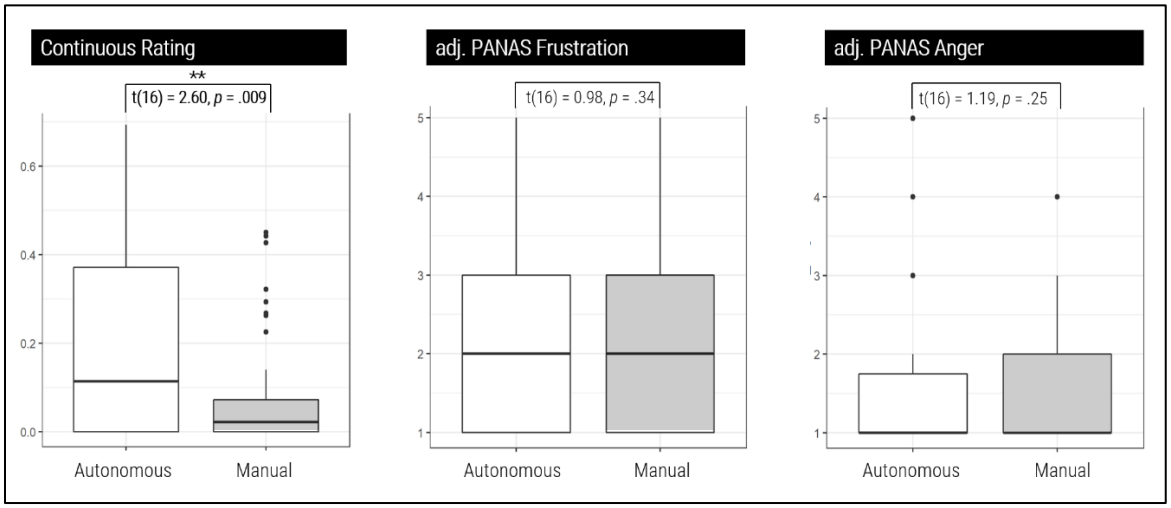

Note: the ratings were averaged over use cases (including baseline and frustration drives)

Taking a closer look at the ratings within the use cases, figures 9 and 10 visualize the (mostly) significant differences of the frustration and anger ratings compared for *baseline* vs. *frustration drives*. The continuous frustration rating in the manual driving scenario and the autonomous driving scenario is significantly different between the conditions, showing that participants were more frustrated within the frustration drives. Equally, for the adjusted PANAS frustration rating in the manual scenario and the autonomous scenario, the rating is significantly higher for frustration drives. There is also a significant difference in the manual drives for the adjusted PANAS rating of anger, which is however not found in the autonomous drives ($p > .05$). This indicates that participants were angrier in the frustration drive in comparison to the baseline drive for the manual driving scenario.

Figure 9 | Frustration and anger ratings for autonomous drives

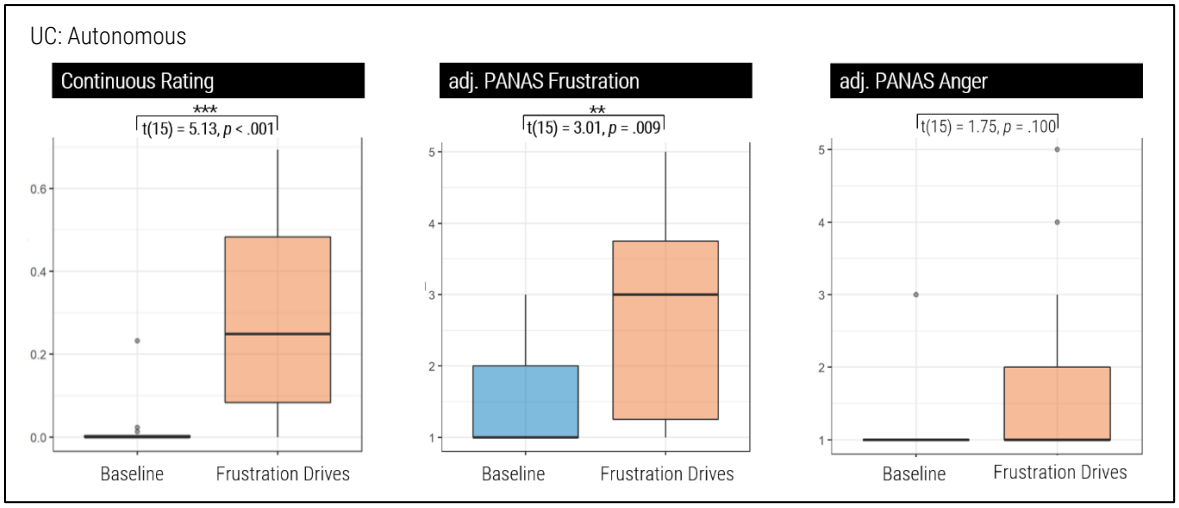

Note: the reduced number of degrees of freedom is due to the missing values of participant (6) for the continuous frustration rating in the baseline drive after artifact removal.

Figure 10 | Frustration and anger ratings for manual drives

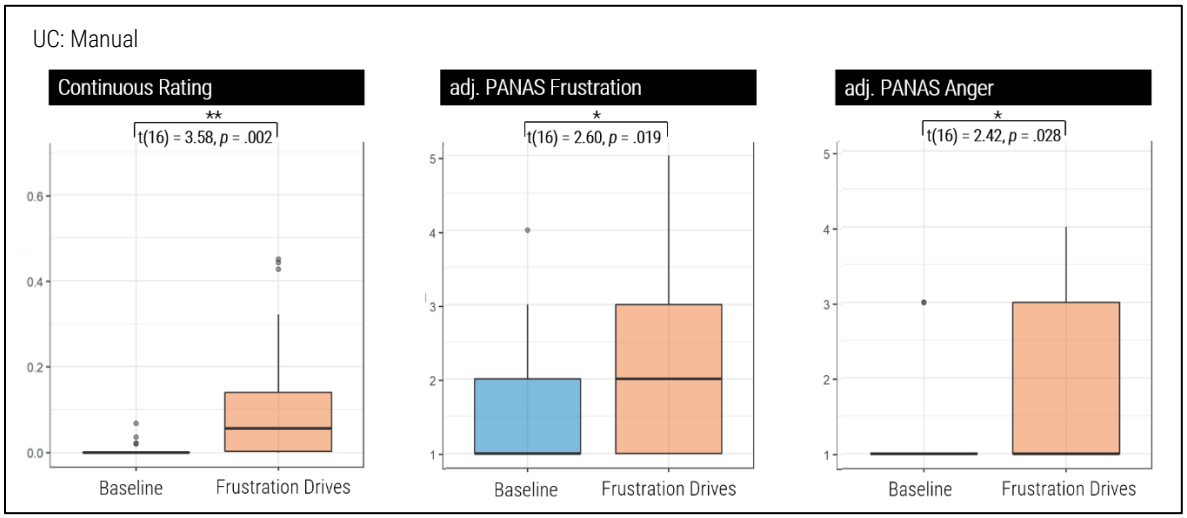

4.2 Visual Inspection

Inspecting the topographical pattern of the frequency band oscillations in relation to the frustration induction overall participants does not indicate significant differences between epochs classified as *no* and *high frustration* (Figure 11). Further, no lateralization effect is visible for the frontal electrodes in the alpha frequency.

Figure 11 | Topographies for the frustration classification

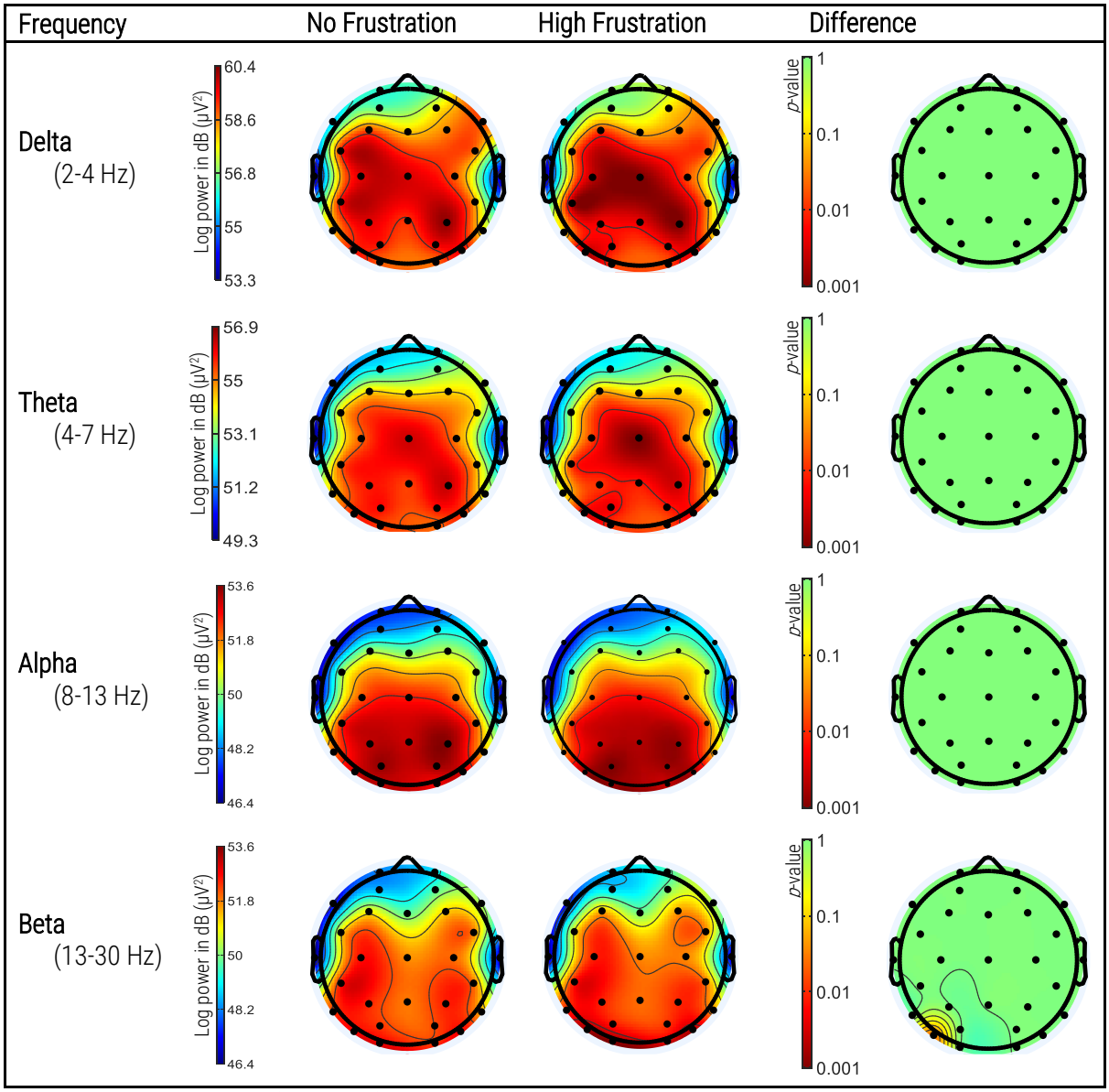

Note: N = 17; missing channels (Appendix A) were interpolated; difference statistics for the effect of the classification (*no* vs. *high frustration*) were corrected with FDR

In addition, the visualization of the spectra for each narrow-band oscillation (*delta, theta, alpha,* and *beta*) averaged over the corresponding electrodes computed by fast *Fourier* transformation only shows minor differences between epochs classified as *no* and *high frustration* (Figure 12).

Figure 12 | Power spectra of narrow-band oscillations

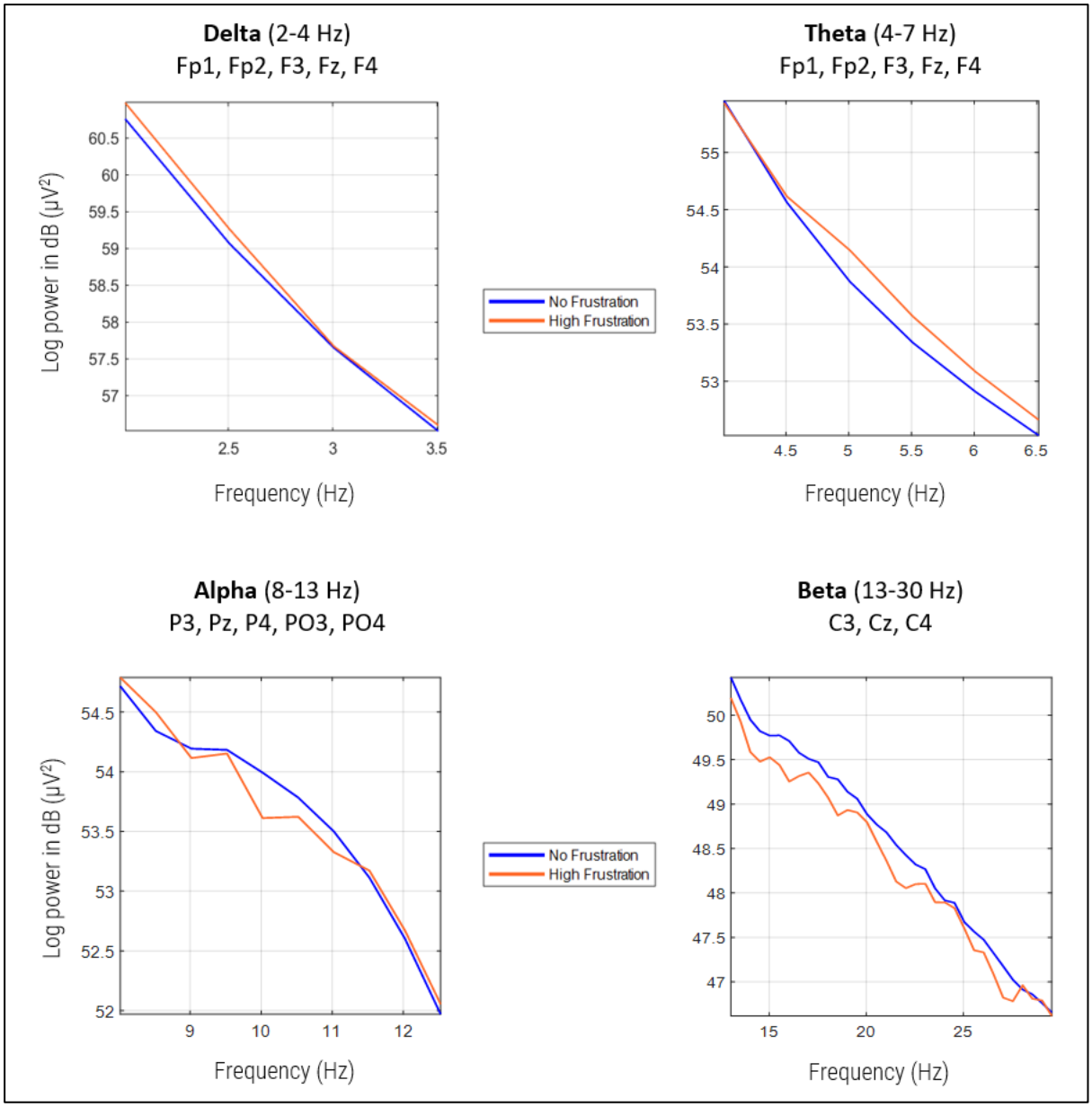

Note: N = 17; spectra are averaged across all participants as well as the specified channels; missing channels (Appendix A) were interpolated

4.3 Frequency band oscillations

Assessing the distribution of measures averaged for participants and category of frustration rating (no frustration vs. high frustration) by a Shapiro-Wilk test, all the logarithmized relative power measures in the frequency bands (delta, theta, alpha, beta) and the AAI are normally distributed ($p > .05$).

Mauchly's test indicates that the assumption of sphericity is violated for the variance of the differences between the frequency bands, $\chi^2(5) = 13.33$, $p < .05$. Consequently, degrees of freedom are corrected using the Greenhouse-Geisser estimates of sphericity ($\varepsilon = .70$).

A repeated-measures ANOVA with mean relative power per participant based on Greenhouse Geisser estimates was used to analyze the interaction of frequency band, use case, and frustration rating (Table 6).

Table 6 | Repeated measures ANOVA of the frequency band, use case, and frustration rating

	df	df error	*F*	*p*
Frequency				
Delta vs. Theta vs. Alpha vs. Beta	2.10	29.43	563.76	**< 0.001**
Frustration Rating				
No vs. High Frustration	1	14	0.25	0.57
Use case				
Manual vs. Autonomous	1	14	0.01	0.69
Frequency * Use Case	2.51	35.08	0.14	0.52
Frequency * Frustration Rating	2.41	33.80	0.41	0.71
Frustration Rating * Use Case	1	14	0.02	0.89
Frustration Ration * Frequency * Use Case	2.17	30.31	0.81	0.46

Note: *N* = 15; Two participants (4, 10) were not included in this analysis due to missing values based on the continuous frustration rating in the frustration drives of the manual use case (participants frustration rating did not exceed their quantile threshold for the classification as *high frustration*). The analysis for the interaction of frequency band, use case, and frustration rating (*no vs. high frustration*) are based on Greenhouse Geisser estimates.

Results show a significant difference in power between the delta, theta, alpha, and beta bands ($p < .001$). However, there is no significant effect of frustration, classified by the dichotomized rating, on the relative power within the frequency bands as can be seen by the non-significant interaction term ($p = .462$). These results suggest that relative power does not differ between the presence and absence of frustration within the autonomous or manual driving scenario. Due to non-significant differences, subsequent post-hoc tests for the effects of specific contrasts were omitted.

To analyze if there were differences in the power of the frequency bands between the baseline and frustration drives (condition), an additional post-hoc repeated-measures ANOVA was performed with frequency band, use case, and condition as within-subject measures. Mauchly's test indicates that the assumption of sphericity is violated for all within-subject measures ($p < .01$). The degrees of freedom are again corrected using Greenhouse-Geisser estimates of sphericity ($.67 < \varepsilon > .80$). Again, only the frequency bands show significant differences in the relative power within the participants ($p < .001$) (Table 7).

Table 7 | Results from a repeated-measures ANOVA for frequency band, use case, and condition

	df	df error	*F*	*p*
Frequency				
Delta vs. Theta vs. Alpha vs. Beta	2.06	30.88	549.96	**< 0.001**
Condition				
Baseline vs. Frustration Drives	1	15	0.63	0.44
Use case				
Manual vs. Autonomous	1	15	0.15	0.70
Frequency * Use Case	1.87	28.10	0.90	0.41
Frequency * Condition	1.79	26.81	0.53	0.60
Condition * Use Case	1	15	> 0.01	0.97
Condition * Frequency * Use Case	1.81	27.08	1.53	0.24

Note. *N* = 16; one participant (6) was not included in this analysis due to missing values for the autonomous baseline drive after artifact removal. The analysis for the interaction of frequency band, use case, and condition (*baseline* vs. *frustration drives*) are based on Greenhouse Geisser estimates.

4.4 Alpha Asymmetry Index

Analyzing the relative activation of the alpha band in electrodes F3 and F4 there is a significant difference between the scores of the AAI in frustration epochs compared to non-frustration epochs (*M* = -0.003, *SD* = 0.006) as indicated by a one-sample, one-sided *t*-test *t*(16) = -1.86 *p* = .041. When comparing the differences in AAI scores between ratings (*no* vs. *high frustration*) in the manual driving scenario (*M* = -0.012, *SD* = 0.022) and the autonomous driving scenario (*M* = 0.006, *SD* = 0.013), it shows that only in the manual drive the AAI is significantly lower in the epochs classified as *high frustration* while in the autonomous driving scenario the scores are higher for epochs classified as *high frustration* (Figure 13).

Figure 13 | Alpha Asymmetry Indices split for use cases

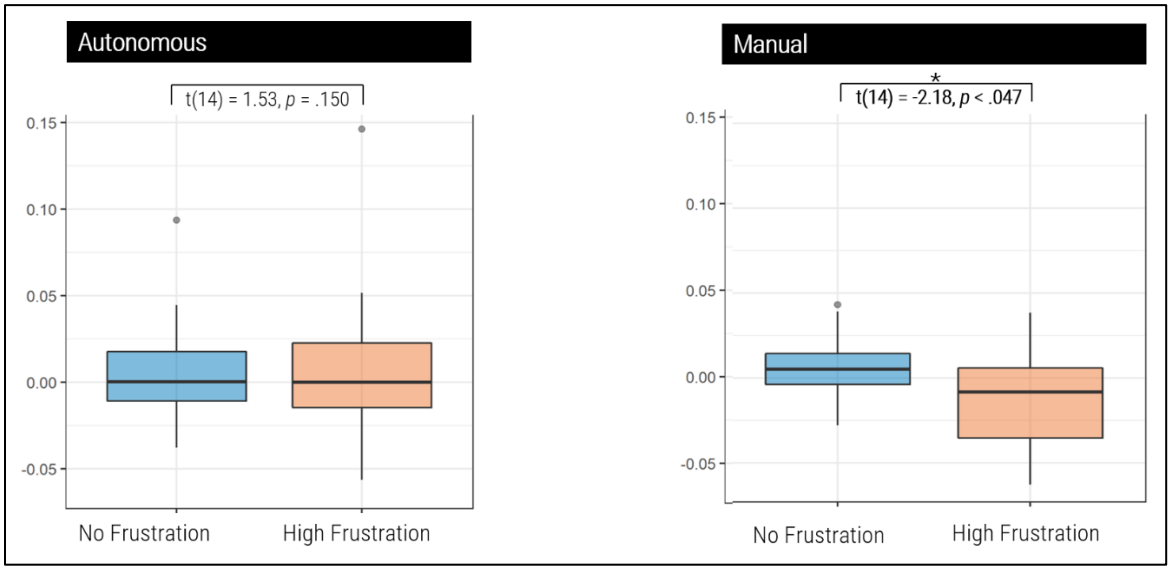

Note. *N* = 15; two participants (4, 10) were not included in this analysis due to missing values based on the continuous frustration rating in the frustration drives of the manual use case (participants frustration rating did not exceed their quantile threshold for the classification as *high frustration*); Alpha Asymmetry Indices are split for use cases and compared between epochs classified by continuous frustration rating (*no vs. high frustration*)

5 Discussion

5.1 Discussion of Alpha Asymmetry Index

This study set out to analyze if frustration induction would lead to the hypothesized lateralization of frontal hemispheres, which would present itself in different power levels of alpha-band oscillations across homologous electrodes along the coronal axis (F4 and F3). It was expected that frustration would elicit more relative left activation within the alpha band and therefore result in more negative AAIs compared to a neutral emotional state (H_{AAI}).

The results for the *Alpha Asymmetry Indices* across use cases show the hypothesized trend of more negative indices for epochs with higher frustration ratings (H_{AAI}). Though unexpectedly, when examining this effect per use case, the hypothesis is only supported by the results of the manual drives. This occurred despite participants rating the manual frustration drives to be far less frustrating than in the autonomous scenario. Likewise, the mean dominance ratings for the manual driving scenario are visibly higher than in the autonomous driving scenario, yet not significant. Simultaneously, the manual driving scenario was rated higher in anger, while there was no significant difference for anger between the conditions within the autonomous drives. Together the ratings are suggesting a possible shift from frustration to anger for the manual driving scenario.

The effect of the higher dominance rating is congruent with recent research showing the dominance dimension to be an important contributor to the lateralization in the frontal cortex (Reuderink et al., 2013; Schuster, 2014; Palmiero & Piccardi, 2017). As is indicated by the higher overall means of the dominance values for the manual use case and their significant correlation with the mean continuous frustration rating, the different effects for the use cases can therefore be contributed to the participant's perception of being more *in control* for the manual use case. This is in concordance with results showing frontal alpha oscillations to be related to the perception of dominance, whereby the feeling of *not being in control* results in more negative Alpha Asymmetry Indices (Grissmann et al., 2017; Reuderink et al., 2013; Schuster, 2014). In addition, some of this research found divergent trends when correlating emotion dimensions within narrower alpha frequencies. Their results are suggesting lower alpha-band oscillations to be corresponding to shifts in valence and upper frequencies to be related to changes in the dominance dimension (Grissmann et al., 2017; Reuderink et al., 2013).

Furthermore, the difference in the dominance rating could reflect the participants' assessment of the attainability for the task at hand. If they perceived the task to be controllable, as in the manual driving scenario, this could have led to an approach motivation, as suggested by Jeronimous and Laceulle (2017). Thereby, the found difference in AAI would reflect the motivational direction of the participants. Support for this explanation is found in the *motivational directional model* (Harmon-Jones & Gable, 2010, 2018).

Nevertheless, the higher values for the dominance rating as well as the adjusted PANAS item for anger give the concerning indication that the found significant difference in the AAI might be in correspondence

to an increase in anger instead of frustration-related effects. This concern is further energized by the research of Harmon-Jones and his colleagues (2006), who found the activation of the relative left frontal cortex to be connected to anger-inducing stimuli.

Apart from the specific underlying emotional dimension, a recent review of the frontal brain asymmetry concluded that the AAI is also dependent on cognitive processes, demographic variables such as age and gender, and general mood of the participants, which would provide an explanation for the inconsistency of effects attributed to the lateralization of frontal brain activity (Palmiero & Piccardi, 2017). Adding to this, the alpha asymmetry score itself is a comparative measure and can therefore emerge by a heightened activation of a single hemisphere as well as a decrease of activity on the contrary hemisphere without being able to differentiate these effects through the score itself (Smith et al., 2017). However, in comparison to other non-relative measures (such as a general increase of power for a specific frequency), a relative measure is more robust, since it can accommodate for an unspecific overall increase or decrease of power resulting from processes that are distinct to the effect of interest.

5.2 Discussion of frequency band correlations

In addition to the analysis of the AAI, the present study explored the correlation of the power in narrow-band oscillations in electrode positions pursuant to the found frustration-classifiers in the study of Myrden and Chau (2017). It was assumed that delta (H_{f1}) and theta (H_{f2}) oscillations would correlate with dichotomized frustration (*no* vs. *high*) at frontal sites, alpha oscillations in posterior positions (H_{f3}), and beta waves in central electrodes (H_{f4}). However, in relation to the dichotomized frustration rating, there were no significant changes detected for the power within these frequency bands at the defined positions. Hence, the found correlations from the algorithm for frustration detection of Myrden and Chau (2017) could not be replicated for the context of frustration within a driving scenario. Since none of the hypothesized effects showed significant results, the hypotheses of the frequency bands ($H_{f1\text{-}4}$) can neither be confirmed nor falsified. Nevertheless, in the subsequent discussion, possible explanations are provided as a rationale for the absence of significant findings by comparison with the state of pertinent research.

For the delta frequency (H_{f1}), comparable research likewise did not find a significant correlation of delta oscillations with a game-related frustration condition (Reuderink et al., 2013). However, significant findings for this frequency have been reported across the entire scalp in relation to a valence condition (positive vs. negative) (Schuster, 2015). Although the manipulation analysis shows clear correlations of the frustration rating with the valence and the dominance dimension, this study could not replicate these results for delta band correlations at frontal electrodes. It must be addressed, however, that in the current study, this frequency band was measured relatively narrowly from 2 to 4 Hz, due to the prevention of aliasing effects from the small time-window (1 second) for the frequency transformation. This in turn was necessary to remove artifacts more precisely. Together with the limited frequency resolution of one Hz, the reliability of the resulting measures is hence questionable. In addition, anterior frontal and temporal areas of this frequency have been reported to be contaminated by the contraction of facial muscles, potentially causing

even more variation of the measure by disturbance of the original brain signals in scalp potentials (Goncharova et al., 2003). Demonstrably, facial muscles such as the *frontalis* and *temporalis* are involved in emotional expressions such as frowning and clenching of the jar. These expressions are commonly observed during episodes of frustration, rendering the activation of these muscles highly momentous for the present study (Goncharova et al., 2003). While similar effects could be present in the study of Myrden and Chau (2017), the fact that their participants were instructed not to move and the stable accuracy of their frustration detection even when leaving out frontal channels speaks in favor of the contrary.

For the theta frequency (H_{f2}), which was decidedly valuable to the cross-subject classification of frustration at the frontal midline position in the study of Myrden and Chau (2017), the summation of the frontal activity in the present study could not find a significant interaction with frustration (H_{f2}). Previous research has found a relation between the emotional valence of a content and theta power at frontal-medial and fronto-lateral sites (Reuderink et al., 2013; Mühl et al., 2014). The power of the fronto-medial theta oscillations has been observed to increase for positive valence induced by pleasant music (in comparison to unpleasant music) as well as with the presentation of emotional (negative, neutral, and positive) film clips (Lee & Hsieh, 2014; Sammler et al., 2007). Researchers even suggested the frontal midline theta to be better suited for emotion-based human-brain-interfaces to detect changes in valence and arousal than the alpha asymmetry (McFarland et al., 2016). Other research suggests emotional changes in valence and dominance dimensions to appear in frontal theta waves in accordance with the lateralization effect (Lin et al.; 2010; Reuderink et al., 2013). Correspondingly, negative emotions have been found to correlate with increased activity of theta oscillations in the right frontal hemisphere and vice versa. In this respect, the summation of all frontal electrodes in the present study would have led to the cancelation of these effects.

Regarding the alpha oscillations (H_{f3}), the contextually similar study of Reuderink and colleagues (2013) (exploring each of 32 electrode sites) found significant changes for frontal (F3, FC1, Fz, CP1) alpha oscillations for different degrees of frustration. Despite this activation appearing to resemble a lateralization effect, the researchers could not find corresponding significant correlations with the dimensions of valence and dominance. However, they did find trends for these dimensions in a more detailed analysis of the alpha band dividing it into 1 Hz partitions. Likewise, Grissmann and colleagues (2017) analyzed the effect for *loss of control* (dominance) in the alpha frequency and found differences in lower and upper alpha band frequencies (decrease and increase respectively for loss of control). Although the manipulation analysis of the present study shows significant correlations of the mean frustration rating with the valence and the dominance dimensions, correlations could not be observed for the relative power in posterior channels amalgamated over the entire alpha band. In conclusion, this suggests that for future research the evaluation of lower and upper alpha oscillation in frontal electrodes could transpire insightful information to the detection of a frustration pattern within this frequency.

Albeit Myrden and Chau (2017) demonstrated posterior alpha to inherit relevant information for their subject-independent frustration classifier training, they observed this feature to be far more predominant

when deploying a subject-dependent classification. This suggests potential individual effects for this measure, which thus would not be prevalent homogeneously between subjects. Supporting evidence for an individual-dependent emotion pattern, beyond the alpha oscillations, is found in numerous affective computing studies, reporting the accuracy of the emotion detection to be superior for individual rather than interindividual models (Hu et al., 2019; Mühl et al., 2014; Petrantonakis et al., 2011; Zhang et al., 2020). The subject-specific emotional representation in the brain is also reinforced by constructionist emotion research, finding emotion categories to be more like fuzzy representations in the brain occurring based on probabilistic processes dependent on context, personality, and prior experience (Barrett, 2017; Clark-Polner et al., 2016; Hoemann et al., 2020). In addition, Myrden and Chau (2017) found the participant-independent classifications to increase in predictive power, when adding more features, assuming this to point towards a population of a few features which possess individuum-specific information for each emotional state. This observation could be linked to the presumed involvement of alpha oscillations in the synchronization of large-scale networks (inter alia the *default mode network*) (Laufs et al, 2006). According to Clark-Polner and colleagues (2016), these networks, in coherence with the assumption of an *affective workspace* in the brain, represent an essential building block for the genesis of conscious emotions. However, the superiority of individual-depended classifications is at least partially owed to the additional emotion-unrelated but confounding variables between the participants and should therefore be interpreted with caution. Nonetheless, together this research implies that a more individualized approach to emotion detection could be advantageous.

Lastly, in contrast to the insignificant power differences in central electrodes (H_{f4}), beta oscillations have previously been found to carry frustration-predictive information in central and frontal positions (Myrden & Chau, 2017). Further beta waves have been shown to correlate (or show trends of such) with reported dominance values at midline electrodes as well as with valence ratings at the left central and right frontal electrodes (Schuster, 2015; Koelstra et al., 2010; Reuderink et al., 2013).

Whereas the increased prevalence of this frequency is often attributed to prolonged attention processes, it is also known to be influenced by muscle artifacts resulting from facial expressions (Soleymani et al., 2016).

While Goncharova and colleagues (2003) found artifacts to manifest over all frequencies, the contamination is described to spread from anterior positions to posterior sites in proportion to rising frequencies. In this light, other studies found similar contamination of facial expressions to be most prevalent in high frequencies such as beta and gamma oscillations (Soleymani et al., 2016). Soleymani and colleagues (2016) took a closer look at the degree to which EEG components were able to predict the valence of emotion above this contamination. They observed facial expression artifacts in the beta band over central and left-sided temporal scalp positions. Nevertheless, they concluded that EEG components were able to explain at least some additional variation within the emotion detection besides the influence from facial muscles alone (Soleymani et al., 2016).

Hence, it is possible that the previous findings for central beta as well as frontal delta oscillations are either despite or even due to these facial expression artifacts, as they plausibly possess emotionally relevant information. This implies that a thorough artifact removal of the EEG data would lead to the elimination of this emotion-relevant information. Here, it becomes necessary to distinguish between possible aims of an EEG measurement. While such artifacts are a hindrance to observe brain-related emotional processes, they could be expedient for affective computing approaches to classify frustration more accurately.

Going forward, the discussion will examine broader aspects concerning the results of the analyses for the effects of frustration on the power within narrow-band oscillations.

Firstly, the most intuitive explanation for the discrepancy of the results in comparison to the underlying research basis of the study from Myrden and Chau (2017) is the already mentioned contamination of the frustration rating with anger-related affective states in the present study. However, the manipulation check only shows significant signs for a commingling of frustration and anger in the manual driving scenario. Thus, taking the use case into account for the analysis comparing frustration effects should have avoided this contamination at least for the autonomous driving scenario.

Secondly, the different situational context in comparison to the frustration induction setting of the experiment from Myrden and Chau (2017) could explain the existing incongruence. This explanation is reinforced throughout dimensional and psychologist construction emotion models, highlighting the dependence of emotional states on the surrounding context (Gross & Barrett, 2011; Scherer, 2005). In addition, it would also explain why the frustration pattern from solving mental tasks in the study of Myrden and Chau (2017) was not found for frustration in the context of driving-simulator-tasks.

Thirdly, a post-hoc power analysis reveals that even with the very conservative presumption that the observable effect of self-reported frustration on the power within each frequency band is strong (r = .5) the power of this effect would still only accumulate to 0.56 with the sample size of this study (Hemmerich, 2018). Optimally, it should achieve a power over .80 to have an appropriate probability of finding an effect if such exists in the population (Sander, et al., 2020). Under the assumption that a true effect of frustration on the power within the frequency bands exists in the general population, the probability of finding this effect in the present study is 44 % (Hemmerich, 2018). For obtaining an appropriate power (0.8) at least 29 participants would have been required, again under the assumption of a strong effect r = .5 (Hemmerich, 2018). In conclusion, future research should, if possible, adhere to this lower limit and ideally even go beyond it to accommodate unexpected participant exclusions.

5.3 Limitations

Regarding the limitations of this study, it must be considered that the experimental design was not oriented towards optimal conditions to measure an EEG, due to the emphasis on the practical application of the research. As a result, the amount of data remaining after artifact rejections ranges from 13 % to 84 % (Appendix A). Unfortunately, removing noise within EEG signals via filters and additional supplementary processes inevitably also distorts the signals of interest (Widmann et al., 2015). Subsequent research in

similar settings could prevent the severity of the distortion by simultaneous measurement of potential artifacts such as facial EMG and EOG information, which can then be used to clean the EEG data specifically of facial and eye movement.

Further, even if the induced emotion is presumed to have been the same instance of frustration for each participant, psychological construction emotion models assume different participant-dependent brain activation patterns based on mood, experience, and cultural contexts (Clark-Polner et al., 2016; Gross & Barrett, 2011; Hoemann et al., 2020). This would imply that the instances of frustration between the two driving scenarios could differ between participants. Likewise, the use of active emotion elicitation, in comparison to standardized stimuli, inherits the possibility of a reduced precision for emotion manipulation (Kory & D'Mello, 2015). Therefore, the active emotion elicitation method and lack of standardization could have led to an increased variability between and within-subjects. In concordance, the limited standardization of electrode placements due to the one-sized EEG system could have further added to a decreased comparability of the effects between the participants.

In addition, the possibility exists that the epochs with the highest frustration had to be excluded from the analysis because the participants might have shown emotion-related facial expressions that would have led to high amplitude noise contamination and consequently to the rejection of these time windows. Support for this assumption can be found in the lower mean quantile threshold across participants after the rejection of noise-laden epochs (0.42 before vs. 0.37 after rejection) (Appendix A).

Furthermore, previous research has shown that the measurement of the subjective account of emotions is limited in manifold ways. For instance, the participants could simply not be aware of their current emotional status or reflective enough to classify the emotion correctly. Barrett (2017) also stresses that a person is only able to classify the emotion for which they have learned concepts and language. Some scientists further assume that especially people with mental disorders, but also the non-clinical population, differs in their interoceptive abilities to perceive their bodily signals and emotions (Barrett et al., 2004; Grabauskaitė et al., 2017). More explicitly, Grabauskaitė and colleagues (2017) have found gender-specific effects on interoceptive abilities. Their results suggest women are better aware of their interoceptive signals and to more frequently relate these to emotional experiences, while men were more accurate in the interoceptive accuracy of reporting their heartbeats. Consequently, future research endeavors could gain additional insights by utilization of interoception measures such as the *Multidimensional Assessment of Interoceptive Awareness* or the *Heartbeat Perception Task* (Mehling et al., 2017; Schandry, 1981) to control for interoceptive abilities of the participants.

Furthermore, the participants showed diverse rating styles for the continuous frustration rating via joystick. While some participants rated their frustration as continuously increasing others only reported short bursts of frustration over time, which additionally were sometimes only small in their amplitude. This led to the choice of using a quantile to classify the rating dichotomously. However, using an interpersonal-specific quantile ultimately results in the equating of potentially very different absolute frustration ratings

for the upper frustration-classification bounds. Whereas, for one person, a mean frustration rating above 0.76 (participant 4) would lead to the classification of *high frustration*, for another the threshold could be 0.36 (participant 6) or even as low as 0.12 (participant 15) (Appendix A). Yet, this methodology seemed to be best tailored to differentiate between individual-specific episodes of highest in comparison to lowest experienced frustration levels.

Likewise, the feature extraction could have been a source of errors. The definition of the one-second time window for the mean of the continuous rating and spectral calculations was merely due to the high number of artifacts within the data. While a longer time window would have provided a superior frequency resolution, it simultaneously would have resulted in the rejection of an intolerable amount of data, as short-timed artifactual bursts in a channels' amplitude would proportionally impact more potentially undisturbed data. As a result, the analysis assumes the post-hoc rating of the participants to be exact for each second of the accumulated one-hour-long drive, which does not seem very plausible, yet was a necessary presumption.

In the following, implications for future research and practical applications are provided based on the insights acquired from these implications.

5.4 Implications

Considering the above-mentioned circumstances, forthcoming studies are needed to build on the current research before such an EEG-based emotion recognition technique for frustration can be used in practical applications.

Those researchers would seemingly be well-advised if they were to couple the emotional state to a time-related stimulus to better inspect the narrow-band oscillations regarding their reflection of the degree of frustration. Further, the experimental design would optimally be constructed in a way that allows extracting trials sufficient in length (optimally 10 - 30 seconds) and stimulus repetitions, which are pinpointed to a distinct frustration-inducing time point. An example for a time-coupled method in a natural setting has been developed by Reuderink and colleagues (2009), who adjusted the "Pacman" game to induce short periods of frustration. Analogously, the approach could be transferred to induce frustration in the driving simulator through the manipulation of the mock-up car's steering wheel or the interaction interface rather than by the driving scenario of the simulated drive itself (frustration vs. baseline drives). Thereby, the data would provide the basis for a higher frequency resolution in the spectral decomposition and could simultaneously be combined with relevant and well-researched EEG components within the time domain. According to Luck (2014), coupling the elicitation of the EEG component of research interest with an already established and well-studied component, such as an ERP, is good practice for the verification of the found effects. In this regard, Spüler and Niethammer (2015) have demonstrated the ERP to be detectable for outcome errors in the time domain (positivity after 300 ms; also called "P3") as well as in the corresponding frequency domain (central delta and fronto-medial theta). Conceivably, the interaction mechanisms (steering wheel and display) could be conceptualized to elicit an ERP (e.g., P3) to the outcome of the participants' action while

simultaneously inducing frustration. In doing so, researchers could check for the presence of this component to verify the frustration elicitation.

Furthermore, the emotional state would optimally be analyzed based on a multi-modal approach evaluating self-rated, behavioral, and physiological measurement simultaneously (for a tutorial and review see He et al., 2020; Zhang et al., 2020).

In Addition, the predictability of frustration could be enhanced by first training a general participant-independent model, which can subsequently be calibrated to individual-specific frustration patterns (Zhang et al., 2020). Hereby the classification features could combine global measures as well as more fine-grained information from single electrodes and narrow-band frequencies.

Moreover, an adaptive frustration induction could prove to be beneficial to subsequent research endeavors for minimizing the possibility of inducing unintended emotions while simultaneously being cautious of the participants' well-being.

Lastly, while the practical implementation of this technology as a way to adapt the human-machine interaction for safer driving still seems to require further development, ethical considerations should already be of importance. As the amount of data generated by each user of sensor-equipped technologies is rapidly increasing, so are the possible privacy concerns. Developers of emotion recognition technologies should therefore already be working on methods to assure that the acquired data will be handled in a way that protects the user's *mental privacy* (Hu et al., 2019; Steinert & Friedrich, 2020).

5.5 Conclusion

This thesis aimed at the detection of an EEG-based pattern of frustration within an ecologically valid setting. It both showcased the underlying methodological theory and summarized relevant trends of the current state of research. Further, details of the methodology have been provided, which were adjusted for the unconventional circumstances concomitant to the practical orientation of this study. The results were accordingly not unambiguously decisive. Although there are studies that found evidence for the reflection of valence in the AAI, the results of this study are in line with the research suggesting the indices to be correlating with feelings on the dominance dimension (Reuderink et al., 2013; Palmiero & Piccardi, 2017). Further, as indicated by a shift in the dominance dimension as well as in the affective rating, a clear commingling of frustration and anger was observed for the condition in which the AAI scores were, as hypothesized, more negative for *high frustration* (in comparison to *no frustration*). Conclusively, the corresponding hypothesis H_{AAI} cannot be regarded as affirmed nor falsified, since the effect is not distinctively attributable to the emotional state of frustration due to increased anger ratings for this scenario. Regarding the yet to be replicated effects of frustration on the narrow-band frequency oscillations partitioned in delta, theta, alpha, and beta waves, the hypotheses $H_{f1\text{-}4}$ could not be confirmed, as they did not show a significantly distinct pattern for frustration at the hypothesized positions (frontal, frontal, posterior and central, respectively). This study represents an exploratory approach for the recognition of frustration in this novel EEG setting. Implications for future research were deducted from the relation of

present results to previous research findings to pave the way for forthcoming research with insights acquired from the present research endeavor. Overall, this thesis aimed to explore the possibilities of EEG-based frustration detection and concludes with suggestions that optimistically prevent frustration for future researchers and developers.

6 References

Aday, J., Rizer, W. & Carlson, J. M. (2017). Chapter 2 - Neural Mechanisms of Emotions and Affect. In Jeon, Myounghoon (Hrsg.), *Emotions and Affect in Human Factors and Human-Computer Interaction* (S. 27–87). Academic Press. https://doi.org/10.1016/B978-0-12-801851-4.00002-1

Affectiva (2021) Affectiva Automotive AI: Redefining the occupant experience and improving road safety with In-Cabin Sensing. https://go.affectiva.com/auto (accessed on August 20, 2021).

Alarcao, S. M. & Fonseca, M. J. (2019). Emotions Recognition Using EEG Signals: A Survey. *IEEE Transactions on Affective Computing*, *10*(3), 374–393. https://doi.org/10.1109/TAFFC.2017.2714671

Alimardani, M. & Hiraki, K. (2020). Passive Brain-Computer Interfaces for Enhanced Human-Robot Interaction. *Frontiers in Robotics and AI*, *7*, Artikel 125. https://doi.org/10.3389/frobt.2020.00125

Al-Nafjan, A., Hosny, M., Al-Ohali, Y. & Al-Wabil, A. (2017). Review and Classification of Emotion Recognition Based on EEG Brain-Computer Interface System Research: A Systematic Review. *Applied Sciences*, *7*(12), 1239. https://doi.org/10.3390/app7121239

Ayata, D., Yaslan, Y. & Kamasak, M. Ayata, D., Yaslan, Y., & Kamasak, M. (2017). Emotion Recognition via Galvanic Skin Response: Comparison of Machine Learning Algorithms and Feature Extraction Methods. Istanbul University. *Journal of Electrical and Electronics Engineering*, *17*, 3129–3136.

Barbosa, L. V. (2013). *Fourier transform time and frequency domains*. https://commons.wikimedia.org/wiki/File:Fourier_transform_time_and_frequency_domains_(small).gif (accessed on July 7, 2021).

Barrett, L. F. (2017). The theory of constructed emotion: an active inference account of interoception and categorization. *Social cognitive and affective neuroscience*, *12*(1), 1–23. https://doi.org/10.1093/scan/nsw154

Barrett, L. F., Quigley, K. S., Bliss-Moreau, E. & Aronson, K. R. (2004). Interoceptive sensitivity and self-reports of emotional experience. *Journal of Personality and Social Psychology*, *87*(5), 684–697. https://doi.org/10.1037/0022-3514.87.5.684

Barrett, L. F., Wilson-Mendenhall, C. D., & Barsalou, L. W. (2013). The conceptual act theory: A road map. Chapter to appear in L. F. Barrett and J. A. Russell (Eds.), *The psychological construction of emotion*.New York: Guilford.

Bennett, C. M., Miller, M. B. & Wolford, G. L. (2009). Neural correlates of interspecies perspective taking in the post-mortem Atlantic Salmon: an argument for multiple comparisons correction. *NeuroImage*, 47, S125. https://doi.org/10.1016/S1053-8119(09)71202-9

Bradley, M. M., & Lang, P. J. (1999). International Affective Digitized Sounds (IADS): Stimuli, instruction manual and affective ratings (Tech. Rep. No. B-2). Gainesville, FL: University of Florida.

Braun, M., Pfleging, B. & Alt, F. (2018). A Survey to Understand Emotional Situations on the Road and What They Mean for Affective Automotive UIs. *Multimodal Technologies and Interaction*, *2*(4), 75. https://doi.org/10.3390/mti2040075

Braun, M., Weber, F. & Alt, F. (2020, 30. März). *Affective Automotive User Interfaces -- Reviewing the State of Emotion Regulation in the Car*. http://arxiv.org/pdf/2003.13731v1

Carter, R., Aldridge, S., Page, M. & Parker, S. (2019). *The human brain book* (American edition. Revised and updated new edition). DK Publishing.

Cellina, F., Bucher, D., Veiga Simão, J., Rudel, R., & Raubal, M. (2019). Beyond Limitations of Current Behaviour Change Apps for Sustainable Mobility: Insights from a User-Centered Design and Evaluation Process. Sustainability, 11(8), 2281. doi:10.3390/su11082281

Chliaoutakis, J. E., Demakakos, P., Tzamalouka, G., Bakou, V., Koumaki, M., & Darviri, C. (2002). Aggressive behavior while driving as a predictor of self-reported car crashes. *Journal of Safety Research*, *33*(4), 431–443.

Cisler, J. M. & Koster, E. H. W. (2010). Mechanisms of attentional biases towards threat in anxiety disorders: An integrative review. *Clinical psychology review*, *30*(2), 203–216. https://doi.org/10.1016/j.cpr.2009.11.003

Clark-Polner, E., Wager, T. D., Barett, L. F. (2016). Meta Analysis, Variation, and the Search for BrainBased Essences in the Science of Emotion. In L. F. Barrett, M. Lewis, & J. M. Haviland-Jones (Eds.), *Handbook of Emotions*. (4th ed., pp. 146-165). The Guilford Press.

Cook, I. A., O'Hara, R., Uijtdehaage, S. H., Mandelkern, M. & Leuchter, A. F. (1998). Assessing the accuracy of topographic EEG mapping for determining local brain function. *Electroencephalography and Clinical Neurophysiology*, *107*(6), 408–414. https://doi.org/10.1016/S0013-4694(98)00092-3

Dan Glauser, E. S. & Scherer, K. R. (2008). Neuronal processes involved in subjective feeling emergence: oscillatory activity during an emotional monitoring task. *Brain topography*, *20*(4), 224–231. https://doi.org/10.1007/s10548-008-0048-3

Dasborough, M. T., Sinclair, M., Russell-Bennett, R. & Tombs, A. (2008). Measuring Emotion: Methodological Issues and Alternatives. In N. Ashkanasy & C. Cooper (Hrsg.), *Research Companion to Emotion in Organizations*. Edward Elgar Publishing. https://doi.org/10.4337/9781848443778.00021

Davidson, R. J. (1993). Cerebral asymmetry and emotion: Conceptual and methodological conundrums. *Cognition & Emotion*, *7*(1), 115–138. https://doi.org/10.1080/02699939308409180

Delorme A. & Makeig, S. (2004). EEGLAB: an open-source toolbox for analysis of single-trial EEG dynamics. *Journal of Neuroscience Methods*, *134*, 9–21.

Dzedzickis, A., Kaklauskas, A. & Bucinskas, V. (2020). Human Emotion Recognition: Review of Sensors and Methods. *Sensors (Basel, Switzerland)*, *20*(3). https://doi.org/10.3390/s20030592

Ekman, P. & Cordaro, D. (2011). What is Meant by Calling Emotions Basic. *Emotion Review*, *3*(4), 364–370. https://doi.org/10.1177/1754073911410740

Ekman, P. & Oster, H. (1979) Facial expressions of emotion. *Annu. review psychology* 30, 527–554.

Ekman, P. E., Friesen, W.V. (2002) Facial Action Coding System (FACS) – Manual. Available online: https://www.paulekman.com/facial-action-coding-system/(accessed on June 27, 2021).

F. Drosch & M. A. Wirtz. (2020). *Dorsch - Lexikon der Psychologie* (19. Aufl.). Hogrefe.

Farnsworth, B. (2019). Facial Action Coding System (FACS)—A Visual Guidebook. Available online: https://imotions.com/blog/facial-action-coding-system (accessed on June 30, 2021).

Fischer, M., Richter, A., Schindler, J., Plättner, J., Temme, G., Kelsch, J., Assmann, D., & Köster, F. (2014). Modular and scalable driving simulator hardware and software for the development of future driver assistence and automation systems. *New Developments in Driving Simulation Design and Experiments*, 223–229.

Garcia, D. (2021). Simpson's rule for numerical integration (https://www.mathworks.com/matlabcentral/fileexchange/25754-simpson-s-rule-for-numerical-integration), MATLAB Central File Exchange. (accessed on June 7, 2021).

Goldstein, R. Z. & Volkow, N. D. (2011). Dysfunction of the prefrontal cortex in addiction: neuroimaging findings and clinical implications. *Nature reviews. Neuroscience*, *12*(11), 652–669. https://doi.org/10.1038/nrn3119

Goncharova, I., McFarland, D., Vaughan, T. & Wolpaw, J. (2003). EMG contamination of EEG: spectral and topographical characteristics. *Clinical Neurophysiology*, *114*(9), 1580–1593. https://doi.org/10.1016/S1388-2457(03)00093-2

Grabauskaitė, A., Baranauskas, M. & Griškova-Bulanova, I. (2017). Interoception and gender: What aspects should we pay attention to? *Consciousness and cognition*, *48*, 129–137. https://doi.org/10.1016/j.concog.2016.11.002

Grissmann, S., Zander, T. O., Faller, J., Brönstrup, J., Kelava, A., Gramann, K. & Gerjets, P. (2017). Affective Aspects of Perceived Loss of Control and Potential Implications for Brain-Computer Interfaces. *Frontiers in human neuroscience*, *11*, 370. https://doi.org/10.3389/fnhum.2017.00370

Gross, J. J. & Feldman Barrett, L. (2011). Emotion Generation and Emotion Regulation: One or Two Depends on Your Point of View. *Emotion Review*, *3*(1), 8–16. https://doi.org/10.1177/1754073910380974

Güntekin, B. & Basar, E. (2007). Emotional face expressions are differentiated with brain oscillations. *International journal of psychophysiology: official journal of the International Organization of Psychophysiology*, *64*(1), 91–100. https://doi.org/10.1016/j.ijpsycho.2006.07.003

Harmon-Jones, E. & Gable, P. A. (2018). On the role of asymmetric frontal cortical activity in approach and withdrawal motivation: An updated review of the evidence. *Psychophysiology*, *55*(1). https://doi.org/10.1111/psyp.12879

He, Z., Li, Z., Yang, F., Wang, L., Li, J., Zhou, C. & Pan, J. (2020). Advances in Multimodal Emotion Recognition Based on Brain-Computer Interfaces. *Brain sciences*, *10*(10). https://doi.org/10.3390/brainsci10100687

Hemmerich, W. (2018). StatistikGuru: Poweranalyse für Korrelationen. Retrieved from https://statistikguru.de/rechner/poweranalyse-korrelation.html (acccessed on 02. July 2021).

Hoemann, K., Khan, Z., Feldman, M. J., Nielson, C., Devlin, M., Dy, J., Barrett, L. F., Wormwood, J. B. & Quigley, K. S. (2020). Context-aware experience sampling reveals the scale of variation in affective experience. *Scientific reports*, *10*(1), 12459. https://doi.org/10.1038/s41598-020-69180-y

Hu, X., Chen, J., Wang, F. & Zhang, D. (2019). Ten challenges for EEG-based affective computing [Brain Science Advances (2096-5958)]. Vorab-Onlinepublikation. https://doi.org/10.26599/BSA.2019.9050005

Huang, D., Guan, C., Ang, K. K., Zhang, H. & Pan, Y. Asymmetric Spatial Pattern for EEG-based emotion detection. In *The 2012 International Joint Conference 2012* (S. 1–7). https://doi.org/10.1109/IJCNN.2012.6252390

Ihme, K., Unni, A., Zhang, M., Rieger, J. W. & Jipp, M. (2018). Recognizing Frustration of Drivers From Face Video Recordings and Brain Activation Measurements With Functional Near-Infrared Spectroscopy. *Frontiers in human neuroscience*, *12*, 327. https://doi.org/10.3389/fnhum.2018.00327

Ioannidis, J. P. A. (2005). Why most published research findings are false. PLoS Medicine, 2(8), e124. https://doi.org/10.1371/journal.pmed.0020124Jasper, H. H. (1958). The ten-twenty electrode system of the International Federation. *Electroencephalography Clinical Neurophysiology*, *10*, 371–375.

Jeon, M. (2017), Emotions in Driving. In M. Jeon (Eds.), *Emotions and Affect in Human Factors and Human-Computer Interaction*. (1st ed., pp. 437-474). Academic Press, Inc., USA.

Jeon, M. (2015). Towards affect-integrated driving behaviour research. *Theoretical Issues in Ergonomics Science*, *16*(6), 553–585. https://doi.org/10.1080/1463922X.2015.1067934

Jeronimus, B. F. & Laceulle, O. M. (2020). Frustration. In V. Zeigler-Hill & T. K. Shackelford (Hrsg.), *Encyclopedia of personality and individual differences* (S. 1–9). Springer International Publishing. https://doi.org/10.1007/978-3-319-28099-8_815-1

Jonsson, I.-M. (2009). "Social and Emotional Characteristics of Speech-Based in-Vehicle Information Systems: Impact on Attitude and Behaviour." PhD diss., Linkoping University.

Kirmizi-Alsan, E., Bayraktaroglu, Z., Gurvit, H., Keskin, Y. H., Emre, M. & Demiralp, T. (2006). Comparative analysis of event-related potentials during Go/NoGo and CPT: decomposition of electrophysiological markers of response inhibition and sustained attention. *Brain research*, *1104*(1), 114–128. https://doi.org/10.1016/j.brainres.2006.03.010

Klug, M. & Gramann, K. (2020). Identifying key factors for improving ICA-based decomposition of EEG data in mobile and stationary experiments. *The European journal of neuroscience*. https://doi.org/10.1111/ejn.14992

Knyazev, G. G. (2007). Motivation, emotion, and their inhibitory control mirrored in brain oscillations. *Neuroscience and biobehavioral reviews*, *31*(3), 377–395. https://doi.org/10.1016/j.neubiorev.2006.10.004

Koelstra, S., Muhl, C., Soleymani, M [M.], Lee, J.-S., Yazdani, A., Ebrahimi, T., Pun, T., Nijholt, A [A.] & Patras, I. (2012). DEAP: A Database for Emotion Analysis Using Physiological Signals. *IEEE Transactions on Affective Computing*, *3*(1), 18–31. https://doi.org/10.1109/T-AFFC.2011.15

Kory, J. & D'Mello, S. (2015). Affect Elicitation for Affective Computing. In *The Oxford Handbook of Affective Computing*. https://doi.org/10.1093/oxfordhb/9780199942237.013.001

Lang, P. J., Bradley, M. M., & Cuthbert, B. N. (2008). International Affective Picture System (IAPS): Instruction manual and affective ratings, Technical Report A-8. Gainesville: The Center for Research in Psychophysiology, University of Florida.

Laufs, H., Holt, J. L., Elfont, R., Krams, M., Paul, J. S., Krakow, K. & Kleinschmidt, A. (2006). Where the BOLD signal goes when alpha EEG leaves. *NeuroImage*, *31*(4), 1408–1418. https://doi.org/10.1016/j.neuroimage.2006.02.002

LeDoux, J. E. (2007). *The emotional brain: The mysterious underspinnings of emotional life* (16th print). Simon & Schuster Paperbacks.

Lee, Y.-C. (2010). Measuring Drivers' Frustration in a Driving Simulator. *Proceedings of the Human Factors and Ergonomics Society Annual Meeting*, *54*(19), 1531–1535. https://doi.org/10.1177/154193121005401937

Lee, Y.-Y. & Hsieh, S. (2014). Classifying different emotional states by means of EEG-based functional connectivity patterns. *PloS one*, *9*(4), e95415. https://doi.org/10.1371/journal.pone.0095415

Leuch, L. (2019). *Choosing your reference – and why it matters*. Brain Products GmbH 2019. https://pressrelease.brainproducts.com/referencing/ (accessed on July 11, 2021)

Lin, Y.-P., Duann, J.-R., Chen, J.-H. & Jung, T.-P. (2010). Electroencephalographic dynamics of musical emotion perception revealed by independent spectral components. *Neuroreport*, *21*(6), 410–415. https://doi.org/10.1097/WNR.0b013e32833774de

Lindquist, K. A., Wager, T. D., Kober, H., Bliss-Moreau, E. & Barrett, L. F. (2012). The brain basis of emotion: a meta-analytic review. *The Behavioral and brain sciences*, *35*(3), 121–143. https://doi.org/10.1017/S0140525X11000446

Luck, S. J. (2014). *An introduction to the event-related potential technique*. *Cognitive neuroscience*. MIT; The MIT Press.

MATLAB 2019b (2019), The MathWorks, Natick.

McFarland, D. J., Parvaz, M. A., Sarnacki, W. A., Goldstein, R. Z. & Wolpaw, J. R. (2017). Prediction of subjective ratings of emotional pictures by EEG features. *Journal of neural engineering*, *14*(1), 16009. https://doi.org/10.1088/1741-2552/14/1/016009

Mehling, W. E., Price, C., Daubenmier, J. J., Acree, M., Bartmess, E. & Stewart, A. (2012). The Multidimensional Assessment of Interoceptive Awareness (MAIA). *PloS one*, *7*(11), e48230. https://doi.org/10.1371/journal.pone.0048230

Mehrabian, A. (1996). Pleasure-arousal-dominance: A general framework for describing and measuring individual differences in Temperament. *Current Psychology*, *14*(4), 261–292. https://doi.org/10.1007/BF02686918

Mishra, S., & Tiwary, U. S. (2019). A Cognition-Affect Integrated Model of Emotion. arXiv: *Neurons and Cognition*. http://arxiv.org/pdf/1907.02557v3

Mühl, C., Allison, B., Nijholt, A. & Chanel, G. (2014). A survey of affective brain computer interfaces: principles, state-of-the-art, and challenges. *Brain-Computer Interfaces*, *1*(2), 66–84. https://doi.org/10.1080/2326263X.2014.912881

Myrden, A. & Chau, T. (2017). A Passive EEG-BCI for Single-Trial Detection of Changes in Mental State. *IEEE transactions on neural systems and rehabilitation engineering: a publication of the IEEE Engineering in Medicine and Biology Society*, *25*(4), 345–356. https://doi.org/10.1109/TNSRE.2016.2641956

Nass, C., Jonsson, I.-M., Harris, H., Reaves, B., Endo, J., Brave, S. & Takayama, L. (2005). "Improving Automotive Safety by Pairing Driver Emotion and Car Voice Emotion." Paper presented at the *SIGCHI Conference on Human Factors in Computing Systems* (CHI05), Portland, OR, April 2-7.

Palmiero, M. & Piccardi, L. (2017). Frontal EEG Asymmetry of Mood: A Mini-Review. *Frontiers in behavioral neuroscience*, *11*, 224. https://doi.org/10.3389/fnbeh.2017.00224

Panksepp, J. (2004) Affective neuroscience: The foundations of human and animal emotions. Oxford University Press.

Posner, J., Russell, J. A. & Peterson, B. S. (2005). The circumplex model of affect: an integrative approach to affective neuroscience, cognitive development, and psychopathology. Development and psychopathology, 17(3), 715–734. https://doi.org/10.1017/S0954579405050340

Reuderink, B., Mühl, C. & Poel, M. (2013). Valence, arousal and dominance in the EEG during game play. *International Journal of Autonomous and Adaptive Communications Systems*, *6*(1), Artikel 50691, 45. https://doi.org/10.1504/IJAACS.2013.050691

Reuderink, B., Nijholt, A. & Poel, M. (2009). Affective Pacman: A Frustrating Game for Brain-Computer Interface Experiments. In A. Nijholt, D. Reidsma & H. Hondorp (Hrsg.), *Lecture Notes of the Institute for Computer Sciences, Social Informatics and Telecommunications Engineering. Intelligent Technologies for Interactive Entertainment* (Bd. 9, S. 221–227). Springer Berlin Heidelberg. https://doi.org/10.1007/978-3-642-02315-6_23

RStudio Team (2019). RStudio: Integrated Development for R. RStudio, Inc., Boston, MA URL http://www.rstudio.com/).

Russell, J. A. & Mehrabian, A. (1977). Evidence for a three-factor theory of emotions. *Journal of Research in Personality*, *11*(3), 273–294. https://doi.org/10.1016/0092-6566(77)90037-X

Russell, J. A. (1980). A circumplex model of affect. Journal of Personality and Social Psychology, 39, 1161–1178. https://doi.org/10.1037/h0077714

Sammler, D., Grigutsch, M., Fritz, T. & Koelsch, S. (2007). Music and emotion: electrophysiological correlates of the processing of pleasant and unpleasant music. *Psychophysiology*, *44*(2), 293–304. https://doi.org/10.1111/J.1469-8986.2007.00497.X

Schandry, R. (1981). Heart beat perception and emotional experience. *Psychophysiology*, *18*(4), 483–488. https://doi.org/10.1111/j.1469-8986.1981.tb02486.x

Scherer, K. R. (2005). What are emotions? And how can they be measured? *Social Science Information*, *44*(4), 695–729. https://doi.org/10.1177/0539018405058216

Schuster, T. J. (2014). "Elektroenzephalographische Erfassung des emotionalen Nutzerzustands in der simulierten Mensch-Maschine Interaktion." PhD diss., Ulm University.

Smith, E. E., Reznik, S. J., Stewart, J. L. & Allen, J. J. B. (2017). Assessing and conceptualizing frontal EEG asymmetry: An updated primer on recording, processing, analyzing, and interpreting frontal alpha asymmetry. *International journal of psychophysiology : official journal of the International Organization of Psychophysiology*, *111*, 98–114. https://doi.org/10.1016/j.ijpsycho.2016.11.005

Soleymani, M., Lichtenauer, J., Pun, T. & Pantic, M. (2012). A Multimodal Database for Affect Recognition and Implicit Tagging. *IEEE Transactions on Affective Computing*, *3*(1), 42–55. https://doi.org/10.1109/T-AFFC.2011.25

Soleymani, M., Asghari-Esfeden, S., Fu, Y. & Pantic, M. (2016). Analysis of EEG Signals and Facial Expressions for Continuous Emotion Detection. *IEEE Transactions on Affective Computing*, *7*(1), 17–28. https://doi.org/10.1109/TAFFC.2015.2436926

Spüler, M. & Niethammer, C. (2015). Error-related potentials during continuous feedback: using EEG to detect errors of different type and severity. *Frontiers in human neuroscience*, *9*, 155. https://doi.org/10.3389/fnhum.2015.00155

Steinert, S. & Friedrich, O. (2020). Wired Emotions: Ethical Issues of Affective Brain-Computer Interfaces. Science and engineering ethics, 26(1), 351–367.

Sutton, S. K. & Davidson, R. J. (1997). Prefrontal Brain Asymmetry: A Biological Substrate of the Behavioral Approach and Inhibition Systems. *Psychological Science*, *8*(3), 204–210. https://doi.org/10.1111/j.1467-9280.1997.tb00413.x

Torres P, E. P., Torres, E. A., Hernández-Álvarez, M. & Yoo, S. G. (2020). EEG-Based BCI Emotion Recognition: A Survey. *Sensors (Basel, Switzerland)*, *20*(18). https://doi.org/10.3390/s20185083

Towers, D. N. & Allen, J. J. B. (2009). A better estimate of the internal consistency reliability of frontal EEG asymmetry scores. *Psychophysiology*, *46*(1), 132–142. https://doi.org/10.1111/j.1469-8986.2008.00759.x

Vallat, R. (2018). Compute the average bandpower of an EEG signal. https://raphaelvallat.com/bandpower.html (accessed on May 16, 2021)

Watson, D., Clark, L. A. & Tellegen, A. (1988). Development and validation of brief measures of positive and negative affect: The PANAS scales. *Journal of Personality and Social Psychology*, *54*(6), 1063–1070. https://doi.org/10.1037/0022-3514.54.6.1063

Watson, D., & Clark, L. A. (1994). The PANAS-X: Manual for the Positive and Negative Affect Schedule-Expanded Form. Ames: The University of Iowa. https://doi.org/10.17077/48vt-m4t2.

Widmann, A., Schröger, E. & Maess, B. (2015). Digital filter design for electrophysiological data--a practical approach. *Journal of Neuroscience Methods*, *250*, 34–46. https://doi.org/10.1016/j.jneumeth.2014.08.002

Zhang, J., Yin, Z., Chen, P. & Nichele, S. (2020). Emotion recognition using multi-modal data and machine learning techniques: A tutorial and review. *Information Fusion*, *59*, 103–126. https://doi.org/10.1016/j.inffus.2020.01.011

Zhao, G., Zhang, Y. & Ge, Y. (2018). Frontal EEG Asymmetry and Middle Line Power Difference in Discrete Emotions. *Frontiers in behavioral neuroscience*, *12*, 225. https://doi.org/10.3389/fnbeh.2018.00225

Appendix A | Table of analysis epochs and resulting quantile threshold

	Before rejection		After rejection		
			Delta Threshold = 250 μV		
Participant / Original	Quantile threshold for 0.6	Total number of epochs:	Quantile threshold for 0.6	Number of epochs: No Frustration	Number of epochs: High Frustration
1/ 30	0.381	2332	0.191	606	104
2/ 31	0.288	2418	0.166	321	321
3/ 33	0.491	2271	0.459	703	158
4/ 34	0.758	2146	0.761	511	216
5/ 35	0.561	2185	0.576	781	303
6/ 36	0.494	2356	0.359	731	72
7/ 37	0.208	2568	0.185	1236	246
8/ 38	0.376	1939	0.353	444	178
9/ 39	0.239	2295	0.312	300	143
10/ 40	0.561	2225	0.613	280	97
11/ 41	0.364	2289	0.319	1218	333
12 /42	0.478	2173	0.335	615	77
13/ 44	0.321	2074	0.246	1054	144
14/ 45	0.499	2460	0.421	227	97
15/ 46	0.135	2540	0.118	427	71
16/ 47	0.166	2394	0.078	2002	18
17/ 49	0.587	2076	0.613	893	240
18/ 50	0.727	2331	0.555	637	230
Mean/sum	0.424	41072	0.370	12986	3048

Note: Participant 16 was excluded from analysis due to a low quantile threshold (0.078)

Appendix B | Table of channel and component rejection per participant

Participant	Channels rejected	ICA components rejected
1/ 30	Fp1	*E:* 1, 3; *M:* 6, 8, 18
2/ 31	F7	*E:* 1, 3; *M:* 7,14, 17, 25
3/ 33		*E:* 1, 3; *M:* 9, 13
4/ 34		*E:* 1, 5, *M:* 3, 9, 15, 18
5/ 35	Fp1	*E:* 1, 2; *M:* 7, 10, 15, 17, 22
6/ 36		*E:* 1, 3; *M:* 8,13, 28
7/ 37	F8, FC6 T7, T8	*E:* 1; *M:* 9, 11, 20
8/ 38		*E:* 1; *M:* 3, 4, 7, 16, 19, 20, 21
9/ 39	Fp2	*E:* 1; *M:* 11, 17
10/ 40		*E:* 1, 3; *M:* 9, 16
11/ 41		*E:* 1, 4; *M:* 9, 11, 13
12 /42	F8, FC6, T7	*E:* 1, 11; *M:* 2, 8, 10 ,11; *CN:* 25
13/ 44	T7	*E:* 1, 5; *M:* 6, 7, 8
14/ 45		*E:* 1, 6; *M:* 10, 14
15/ 46	Fp1, Fp2	*E:* 1 5; *M:* 11, 12, 19
16/ 47	Fp1	*E:* 1, 3; *M:* 2, 4, 5, 6, 8, 14, 16, 17
17/ 49	PO8	*E:* 1, 3; *M:* 4, 9 ,17,18, 19; *CN:* 11
18/ 50	Fp1	*E:* 1,3, *M:* 14, 18

Note: Participant 16 was excluded from analysis; *E* = eye-related component; *M* = muscle-activity-related component; *CN* = channel-noise-related component